

* * * * *
*
* AFTEREFFECTS, ADAPTATION, AND PLASTICITY: *
* A NEURAL MODEL FOR TUNABLE FEATURE SPACE *
*
* Fanya S. Montalvo *
*
* COINS Technical Report 76-4 *
*
* September 1976 *
*
* * * * *

COMPUTER AND INFORMATION SCIENCE

UNIVERSITY OF MASSACHUSETTS AT AMHERST
AMHERST, MASSACHUSETTS 01002
U.S.A.

(c) Fanya S. Montalvo 1976
All Rights Reserved

Supported, in part, by:

NIH Grant No. 5 R01 NS09755-4 COM
of the National Institute of Neurological
Diseases and Stroke (M.A. Arbib, Principal
Investigator).

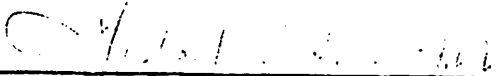
AFTEREFFECTS, ADAPTATION, AND PLASTICITY:
A NEURAL MODEL FOR TUNABLE FEATURE SPACE

A Dissertation Presented


By

FANYA S. MONTALVO

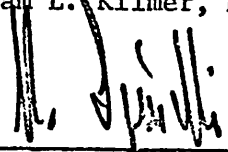
Approved as to style and content by:



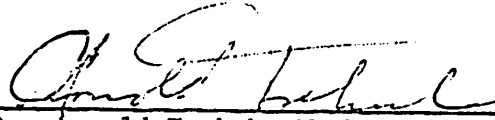
Dr. Michael A. Arbib, Chairperson of Committee



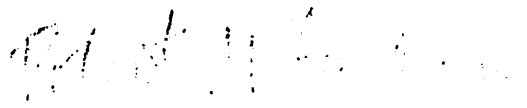
Dr. William L. Kilmer, Member



Dr. D. N. Spinelli, Member



Dr. Arnold Trehub, Member



Dr. Robert M. Graham, Department
Chairperson,
Computer and Information Science
Department

A C K N O W L E D G E M E N T S

Any large and worthwhile project is impossible without the support and encouragement of many people. You can't do it alone. And so it is with great pleasure and humility that I gratefully acknowledge all these kind, helpful, brilliant, and inspiring souls that got me through these last four years.

I thank the woman who first implanted in me the desire to know about "those pictures inside the head," Naomi Weisstein, for her encouragement and faith in me. I thank Michael Arbib for providing the intellectual, financial and spiritual environment that makes the study of brain theory not only possible but satisfying. I thank Bill Kilmer, Nico Spinelli, and Arnold Trehub for their encouragement, understanding, guidance and intellectual support. I thank Charles Harris, Christoph von der Malsburg, and Shun-ichi Amari for their guidance and encouragement of my ideas. I thank Art Karshmer for his emotional and software support, Elliot Soloway for making the department a more human place, Ed Riseman for his inspirational and intellectual support, Caxton Foster for bolstering my technical expertise, Janet Turnbull and Donna Jerkovich for their secretarial support, and the University of Massachusetts Computer Center for their software and hardware support.

Finally, but not without deep appreciation, I thank Jim Stanley for his tireless, humorous and never ending support and encouragement for the love and pursuit of science.

ABSTRACT

Aftereffects, Adaptation and Plasticity:
A Neural Model for Tunable Feature Space

(September 1976)

Fanya S. Montalvo, B.S., Loyola University
Ph.D., University of Massachusetts

Directed by: Dr. Michael A. Arbib

Aftereffects, adaptation, and developmental plasticity are seen as several aspects of synaptic modification, which is a transformation of an internal feature space represented by populations of feature detectors. Techniques in computer image processing such as feature extraction and histogram uniformization are compared to the biological phenomenon of developmental plasticity and aftereffects. Computationally they are very similar and form part of a wide spectrum of feature transformation operations, defined as mappings from a physical feature space to an internal (system) feature space representation. The types of transformations enabled by synaptic modification in neural networks are investigated with computer simulation.

A self-organizing, feature-extracting network (von der Malsburg, 1973) is extended to two feature dimensions to encompass line orientation and color. It is applied to McCollough effects, particularly long-lasting, contingent-aftereffects. McCollough effects are thought to involve low-level associative memory in the form of synaptic modification. The McCollough-Malsburg Model (MMM) embodies positive synaptic modification with correlated firing of units in an input layer and an excitatory cortical layer. Computer simulation of MMM reproduces orientation-contingent color aftereffects. The model embodies many of

the mechanisms thought to be operating in developmental plasticity, suggesting that equivalent mechanisms may be involved in adult long-term adaptation as well.

TABLE OF CONTENTS

	PAGE
LIST OF TABLES.....	ix
LIST OF FIGURES.....	x
I. INTRODUCTION.....	1
1.1. Measuring Visual Features.....	1
1.2. Contingent Aftereffects.....	3
II. TUNABLE FEATURE DETECTORS.....	6
2.1. Biological Evidence.....	6
2.1.1. Plasticity in Development.....	6
2.1.2. Plasticity in Adulthood.....	7
2.1.3. Aftereffects and Adaptation.....	9
2.1.4. The Model in One Dimension.....	11
2.2. Applications in Image Processing.....	24
2.2.1. Segmentation.....	25
2.2.2. Tuning.....	27
2.2.3. Clustering.....	29
III. SIMULATION OF THE McCOLLOUGH-MALSBERG MODEL (MMM).....	34
3.1. von der Malsburg's Model.....	34
3.2. A Color Version of Malsburg.....	36
3.2.1. Some Initial Attempts at Color Coding.....	37
3.2.2. f_2 Version.....	38
3.2.3. f_3 Version.....	48
3.2.4. f_4 Version.....	52
3.3. Eliminating the Synaptic Conservation Rule.....	57
3.3.1. ME's in the Untrained Network.....	60

TABLE OF CONTENTS

	PAGE
3.3.2. Attenuation of Feedback from E-Cells.....	63
3.3.3. Specific Threshold Elevation.....	64
3.4. Model Modelling.....	66
IV. CONTINGENT-AFTEREFFECTS MODELS.....	70
4.1. Are Color and Form Coded Separately or Together?....	70
4.2. Form-Specificity.....	71
4.3. Is Color a Dimension?.....	77
APPENDIX A.....	82
APPENDIX B.....	84
APPENDIX C.....	86
BIBLIOGRAPHY.....	90

LIST OF TABLES

TABLE	PAGE
3.1 Parameters.....	42
3.2 The response of MMM with color coding f_2 to white test stimuli ($v = .5$) before and after alternate hue-orientation presentations.....	47
3.3 The response of MMM with color coding f_3 to white test stimuli ($v = .5$) before and after alternate hue-orientation presentations.....	51
3.4 The response of MMM with color coding f_4 to white test stimuli ($v = .5$) before and after alternate hue-orientation presentations.....	54
3.5 The response of MMM with color coding function f_2 to white test stimuli ($v = .5$) before and after alternate hue-orientation presentations, starting from a spatially untrained network.....	62

LIST OF FIGURES

FIGURE		PAGE
2.1	A uniform distribution of response curves, spaced evenly throughout a feature dimension, with equal tuning widths, $\omega = .5$	13
2.2	The changes in the total activity and featural response produced by shifting of individual response curves, toward the modifying stimulus.....	16
2.3	The changes in the total activity and featural response produced by decrease of individual tuning curve widths near the modifying stimulus.....	17
2.4	The changes in the total activity and featural response produced by increase of individual response curve heights near the modifying stimulus.....	18
2.5	The changes in the total activity and featural response produced by increase of individual response curve thresholds near the modifying stimulus.....	19
2.6	The changes in total activity and featural response produced by shifting, narrowing, and heightening of individual response curves near the modifying stimulus.....	20
2.7	The changes in the total activity and featural response produced by shifting, narrowing, and heightening of individual response curves and increasing of thresholds near the modifying stimulus.....	21
2.8	The changes in the total activity and featural response produced by shifting, narrowing, and heightening of individual response curves near the modifying stimulus.....	23
2.9	Histogram uniformization.....	28
2.10	Clustering.....	31
3.1	Side view of hexagonal input and cortical arrays showing the connectivity between and within the layers.....	35
3.2	Weighted input from red and green opponent-color cells corresponding to color coding function f_1	39

LIST OF FIGURES

FIGURE		PAGE
3.3	Red/green synaptic pair response to saturation, v , corresponding to color coding function f_2	41
3.4	Histogram of cells plotted at their preferred saturation and orientation values using color coding function f_2 and synaptic weights assigned uniformly over synapses.....	43
3.5	Nine line orientations presented to the input layer (R).....	45
3.6	Hypothetical interneuronal circuitry to convert green saturation, $1-v$, and red saturation, v , into color coding function f_3 , by multiplying the outputs of interneurons with sigmoidal responses, \mathcal{S}_g and \mathcal{S}_r	50
3.7	Histogram of cells plotted at their preferred saturation and orientation values using color coding f_4 and synaptic weights assigned uniformly over cells.....	56
3.8	The saturation response for color coding f_4 , with 10 blocks of uniform training.....	58
3.9	Histogram of cells plotted at their preferred saturation and orientation values showing the response to line 4, $v = 1$	59
3.10	The saturation response for color coding, f_0 , with threshold elevation, gain $g = 7.$, and 4 blocks of uniform training.....	65
3.11	The changes in the total activity and featural response produced by shifting, narrowing, and heightening of individual response curves near the modifying stimulus.....	68
4.1	The response of bar detectors the same width as the squares in a checkerboard pattern when aligned orthogonally minus their response when aligned diagonally to the pattern (dashed line).....	75
4.2	The saturation dimension can be thought of as a collapsed, pure color, wrap-around dimension in which blue and yellow coincide to produce white ($v = .5$), and green ($v = 0$) and red ($v = 1$) are located at the extremes.....	79

LIST OF FIGURES

FIGURE	PAGE
4.3 Two parametric experiments to test for tuning width along the color dimension.....	80

CHAPTER I

INTRODUCTION

1.1. Measuring Visual Features

The visual system is an expert at measuring differences. Movement, edges, borders between regions, and flicker are all changes of features in the visual input. Lateral inhibition and temporal inhibition seem designed to amplify small differences and measure derivatives of luminance across space and time as well as other more complex features such as color, line orientation, size, and texture. Measurement of a perceptual feature of any kind must be based on a comparison.

What kind of comparisons are possible in nervous tissue? Whether a cell is on or off is certainly one type, but a finer discrimination measures the relative rates of firing of units in a network. The units making the discriminations are units of the same kind that can distinguish incoming signals only by the set of lines on which those signals arrive or by fluctuations in time. The discriminating units have no way of knowing the characteristics of the receptors that first received the signals from the outside. All they know is that line 1 or line 2 is active and by how much. How do they make the comparison?

The model of contingent-aftereffects proposed in Chapter III assumes that visual feature dimensions are measured by arrays of interconnected elements in terms of the relative firing rates of spatially distinct elements labeled by the feature giving their maximum response. Single cell response curves to a given feature are

assumed to be unimodal. For example, if a cell fires maximally to a line tilted 15° left of vertical then that is its label along the orientation dimension. The network's output measure of a given input feature is based on the average label weighted by unit activity. This measure disregards total activity and variations in the spread (variance) of activity among units ordered by their labels but focuses simply on the mean feature signaled by the population. This measure defines a mapping from the physical feature space to an internal feature space. In general, the mapping is dynamically dependent on the distribution of inputs in the physical space to which the network has been exposed. How this feature mapping is initialized and transformed is the subject of this study.

In Chapter II a featural response measure is defined for an abstract feature dimension. Examples of modifying mechanisms and their effects on the featural response are given. A review of some of the biological evidence for an internal, adaptive, feature space initialized during development and refined throughout life appears. Applications of an adaptive feature space in image processing are briefly summarized.

The McCollough (1965) effect (ME) is particularly interesting from the standpoint of feature definition and tunability because it exhibits modifiability along two dimensions: color differences contingent on orientation and orientation differences contingent on color (Held and Shattuck, 1971). The explanation developed in this thesis is that these differences represent local changes in the visual system's scaling of the physical feature space. A geometrical representation of the internal feature space illustrates these

changes for one dimension in Chapter II and for the two-dimensional ME in Chapter III.

1.2. Contingent Aftereffects

A contingent aftereffect, of which the ME is one example, is a change in the perceived value of a visual feature dimension, such as color, contingent on the value of another feature dimension, such as line orientation. Stated more concretely, the ME is produced by viewing vertical red and black stripes and horizontal green and black stripes alternating every 5 or 10 seconds for about 5 minutes or more. After these adaptation presentations a vertical black and white test grating will appear slightly green while a horizontal black and white test grating will appear pink. The effect can also be induced by red and green vertical gratings of two different spatial frequencies (Stromeyer, 1972a), and by gratings of complementary colors moving in opposite directions (Hepler, 1968; Stromeyer and Mansfield, 1970; Mayhew and Anstis, 1972). The effect depends on retinal spatial frequency (Teft and Clark, 1968) rather than on viewing distance (Harris, 1971). The effect does not depend on retinal fixation necessary for afterimages (Harris and Gibson, 1968a), but only on general retinal location (Stromeyer, 1972b). It is also unlike afterimages in its long duration, sometimes on the order of hours, days or even weeks depending on the length of adaptation (Stromeyer and Mansfield, 1970; Mayhew and Anstis, 1972; Riggs, White and Eimas, 1974; MacKay and MacKay, 1975).

In addition to its decay rate being very long with respect to afterimages, the decay also appears to depend on stimulation after

adaptation. Black and white gratings (Skowbo, et. al., 1974) and diffuse light (MacKay and MacKay, 1975) were found to reduce the effect at a faster rate than mere darkness. In fact, MacKay and MacKay found no decay of the effect after periods of darkness and Mayhew and Anstis (1972) reported a slight increase in the effect after 20 minutes of rest. No reported single-unit fatigue or inhibitory rebound behaves in this manner. It is unlikely that fatigue of single units can last for weeks.

Although orientation, spatial frequency, and movement aftereffects transfer interocularly (Blakemore and Campbell, 1969; Gilinsky and Doherty, 1969; Lovegrove, Over and Broerse, 1972), color aftereffects contingent on these features do not under usual transfer paradigms (Stromeyer and Mansfield, 1970; Maudarbocus and Rudock, 1972; Murch, 1972; Lovegrove and Over, 1973). MacKay and MacKay (1973) produced some binocular interaction with form and color presented separately to both eyes, but Over, Long and Lovegrove (1973) with a similar paradigm did not find such interaction. However, Over, et. al., used verbal reports not a quantitative null-method for measuring the aftereffect, and measured the effect with both eyes. If opposite effects are built up in the two eyes, as the MacKays had found, the effects would cancel. In the same study, Over and his colleagues were unable to induce a color aftereffect contingent on binocular disparity. A recent study by Keith White (1976a) indicates that ME's can transfer under conditions of minimal rivalry between the two eyes. Binocular interaction favors a central rather than peripheral mechanism.

Because of its very long decay rate, its dependency on post-adaptation stimulation, and its contingency on spatial frequency, orientation and direction of movement, which indicate a more central rather than peripheral effect, many investigators (Skowbo, et. al., 1975) have gravitated toward some form of an associative learning model to explain the effect. However, an associative learning model has trouble accounting for a color aftereffect complementary to that paired with specific spatial information during adaptation. The usual way of explaining a negative aftereffect is that an opponent-color neutralizing response is associated with the spatial stimulation during adaptation (Kohler, 1962; Leppman, 1973). Creutzfeldt (1973) has suggested a model involving correlated incrementation of inhibitory synapses between reverberating color and line orientation cells in cortex, but elevated thresholds for orientation- and color-specific stimuli have not been demonstrated during ME (Timney, et. al., 1974). The neural network simulation presented in Chapter III demonstrates that the ME can be obtained by using incrementation of excitatory synapses between two layers. The model embodies many of the mechanisms thought to be involved in the development of line orientation detectors in young animals (von der Malsburg, 1973) suggesting that these mechanisms may be operating in adult long-term adaptation. The network is meant to model qualitative aspects of the transformation of an internal feature space representation, rather than quantitative aspects of the decay rate of the aftereffect.

CHAPTER II

TUNABLE FEATURE DETECTORS

2.1. Biological Evidence

2.1.1. Plasticity in Development

A number of studies have shown that there exists a critical period in the development of binocular animals during which the input distribution of visual features influences the distribution of feature detectors in visual cortex. The pioneering study was done by Wiesel and Hubel (1963) by suturing an eyelid of a kitten before visual experience. The suturing totally disrupted the kitten's distribution of ocular dominance. All cells in visual cortex were driven by the normal eye only. Since then early selective experience has been found to affect the distribution, responsiveness, and tuning characteristics of cells sensitive to many other visual features, such as line orientation (Blakemore and Cooper, 1970; Hirsch and Spinelli, 1970; Freeman and Pettigrew, 1973), size and shape (Pettigrew and Freeman, 1973), motion (Cyander, Berman, and Hein, 1973), direction of motion (Pettigrew, 1974a), and retinal disparity (Pettigrew, 1974b). In all of these studies the long-term effect of such exposure is an increase in the number, specificity, and responsiveness of cells sensitive to the feature predominant in the early experience and a decrease in the number, specificity, and responsiveness of cells not tuned to the conditioning feature. Young and inexperienced visual systems possess many weakly responsive or non-responsive cells, easily habituated, with broad tuning curves

(Barlow and Pettigrew, 1971; Blakemore and Mitchell, 1973; Pettigrew, 1974b). Visual exposure sharpens specificity and increases responsiveness to the feature experienced.

2.1.2. Plasticity in Adulthood

After the critical period when detectors are most changeable, even by very short periods of exposure (Blakemore and Mitchell, 1973), there remains some degree of plasticity. In kittens reared under monocular exposure no binocular cells were found after the rearing period. Well after the critical period these cats were exposed to a normal binocular visual environment and developed a large proportion of binocular cells (Spinelli, et. al., 1972). Adult cats exposed to vertical gratings exhibit a distribution of orientation detectors with reduced numbers of units sensitive to vertical (Creutzfeldt and Heggelund, 1975). Spinelli and Metzler (1976) found an increase in the number of cells sensitive to the visual features to which normal adult cats had been exposed. These cats also exhibited better behavioral discrimination of the features present during exposure (Metzler and Spinelli, 1976). The study by Spinelli and Metzler differed from that of Creutzfeldt and Heggelund by having a longer consolidation period before examination.

Although the direction of long-term effects is not clear, plasticity within bounds can be found in adult visual systems. Short-term adaptation effects are largely negative in nature, i.e., exposure reduces sensitivity to the conditioning stimulus, but long-term effects are not clearly negative or positive but may be either depending on the aspect of the aftereffect measured, the length of time

after exposure the test occurs, and the age and experience of the animal. Seconds after exposure, for instance, adaptation to a specific spatial frequency and orientation raises the contrast threshold to the same stimulus (Blakemore and Campbell, 1969; Maffei, Fiorentini and Bisti, 1973). In adult cats exposed only to vertical bars 2 hours/day for 14 days Creutzfeldt and Heggelund (1975) recorded 10 to 20 hours after exposure. They found decreased numbers of units sensitive to vertical. Spinelli and Metzler (1976), however, recorded over a 2 week period from cats exposed to vertical bars in one eye and horizontal bars in the other eye for 6 hours/day over a 6 week period. These cats exhibited increased numbers of units sensitive to the conditions of exposure. Pettigrew's (1974a) study of an inexperienced kitten at its maximum time of plasticity clarifies the differing time course of negative versus positive aftereffects. A 4 week old kitten was prepared for recording and then one eye was exposed to a vertical grating moving leftward for 20 hours. For the first four hours following exposure cells were difficult to drive, had high spontaneous rates of activity, and were inhibited by the conditioning stimulus. However, 8-10 hours after exposure a number of briskly responding cells appeared. Their preferred orientation was vertical and preferred eye was the exposed one. One would expect positive and negative effects to be qualitatively similar in adult animals but perhaps develop over different lengths of time.

Not only is the duration of exposure versus the time of testing crucial to the direction of the effect, but also the method of testing determines what aspect of the effect, positive or negative, will come to light. Most experiments with kittens report increased numbers of

units sensitive to the conditioning stimulus. Presumably, units have become tuned to the input, but this says nothing about the total activity of these units in response to their preferred input. Maffei and Fiorentini (1974) found a reduced amplitude in cortical evoked potentials specific to the spatial frequency to which kittens had been exposed. Specific tuning to a stimulus can lower the overall output activity of a network while increasing the number of units sensitive to that input. The simulation in section 2.1.4. illustrates these apparently contradictory results.

2.1.3. Aftereffects and Adaptation

Exposure to a feature reduces sensitivity to that stimulus for several seconds but also affects the appearance of nearby features along the same dimension for longer periods of time. Nearby features appear less like the adaptation stimulus than they did before exposure. Movement aftereffects, inducing apparent motion in the direction opposite to that of the adaptation stimulus, generated by 15 minutes of exposure can last 20 hours or more (Masland, 1969). Blake-more and Sutton (1969) found that spatial frequencies above and below the adaptation frequency appeared respectively higher and lower than they actually were, for many hours after exposure. As indicated in Chapter I, the ME can last for days or even weeks in some cases and is not necessarily accompanied by reduced sensitivity specific to both the color and orientation of the adaptation stimuli.

Coltheart (1971) and Over (1971) make excellent cases for the assumption that visual features are measured by a weighted average of outputs of a population of feature detectors. Implicit in this

assumption is that visual features belong to one of several continuous feature dimensions, that feature detectors have unimodal tuning curves of some specified width over some dimension, and that a unit's activity represents that feature which produces its maximum response. Feature detectors with such tuning characteristics have been observed neurophysiologically for orientation, color, disparity, spatial frequency, and direction of movement (Over, 1971).

Coltheart and Over's explanation of negative aftereffects is that the population that fires to the adaptation stimulus becomes less sensitive. Viewing a nearby feature following exposure produces an asymmetrical response biased in the direction of the unexposed cells. They distinguish adaptation from negative aftereffects in order to claim that only negative aftereffects are explained by this model. Adaptation is defined as the process by which a stimulus approaches a standard, i.e., a tilted line appears more vertical, while the stimulus is still on. A negative aftereffect is produced after the adaptation stimulus is turned off. I have been using the term "adaptation stimulus" rather loosely as meaning any stimulus that produces aftereffects. Note that aftereffects may occur without adaptation in the above formulation because not all feature dimensions have a standard. Adaptation cannot be explained by reduced sensitivity unless there are units that signal deviation from a standard.

Several other problems with the reduced sensitivity hypothesis arise. No unit recovery curves that persist for hours have been observed physiologically (MacKay, 1973). Threshold elevation specific to spatial frequency and orientation is relatively short (Blakemore, Nachmias and Sutton, 1970; Timney, et. al., 1974). Adaptation is not

accompanied by a steady reduction in unit response after an initial transient, and cells can exhibit aftereffects without being activated by the adaptation stimulus (Maffei, Fiorentini, and Bisti, 1973). Finally, prolonged exposure greatly increases the duration of aftereffects without affecting their magnitude (Gibson, 1933; McCollough, 1965; Blakemore and Sutton, 1969). A word of caution should be inserted, however, about the failure to find prolonged periods of reduced sensitivity along with feature distortion. Studies testing for reduced sensitivity have generally not prolonged the exposure time beyond a few minutes (Blakemore, Nachmias and Sutton, 1970).

The following analysis and simulation along one abstract feature dimension shows that synaptic modification of the sort thought to be present during development can exhibit many of the characteristics present in both adaptation and negative aftereffects. Threshold elevation may be present in their early stages but is not a necessary concomitant of featural aftereffects.

2.1.4. The Model in One Dimension

Visual experience sharpens the tuning characteristics of detectors distributed continuously throughout a feature dimension. Development can be said to define a set of detectors $\{D_i\}$ along a feature dimension, $v \in [0,1]$, with unimodal response curves, each with a specified width, $2\omega_i$, centered at some $v = x_i$, with maximum activity, h_i , and a threshold, θ_i . The exact shape of the tuning curve is not crucial to the analysis as long as it is unimodal. Contrast enhancement of activity in a network with strong inhibition produces a sharp cutoff

at the threshold. The shape of a quadratic represents this general behavior:

$$a_i(v) = [h_i(1 - [\frac{v - x_i}{\omega_i}]^2) - \theta_i]^+ \quad (2.1)$$

The function $[x]^+ = x$ whenever $x > 0$ and $[x]^+ = 0$ otherwise. Figure 2.1 illustrates a distribution of unit response curves having equal widths, heights, and thresholds and having x_i 's distributed evenly throughout v . Suppose that D_i is labeled by the feature, $f_i = x_i$, sometime during development, such that the activity of D_i now represents f_i . This could happen as soon as the tuning curve a_i for D_i gets sharp enough, whenever some threshold value for h_i versus ω_i is reached. Then the label, f_i , fixed by the peak response, $a_i(f_i) \geq a_i(v)$ for all $v \in [0,1]$, is assigned to D_i . Although this tuning curve can be modified by exposure to v , one would not expect the feature that D_i represents to change very easily. The system has no way of determining which v produces the maximum response from D_i . Once the labels are fixed the response to a feature, v , can be determined by the average label weighted by unit activity:

$$R(v) = \frac{\sum_i a_i(v) f_i}{\sum_i a_i(v)}, \quad (2.2)$$

which defines a mapping from the physical feature space to an internal feature space representation.

In general, visual experience throughout development and adult life can modify the characteristics of the distribution $\{a_i\}$. Positive synaptic modification of afferent fibers to D_i can induce three types of modification, provided that synaptic growth is limited either by conservation of total strength (von der Malsburg, 1973) or by

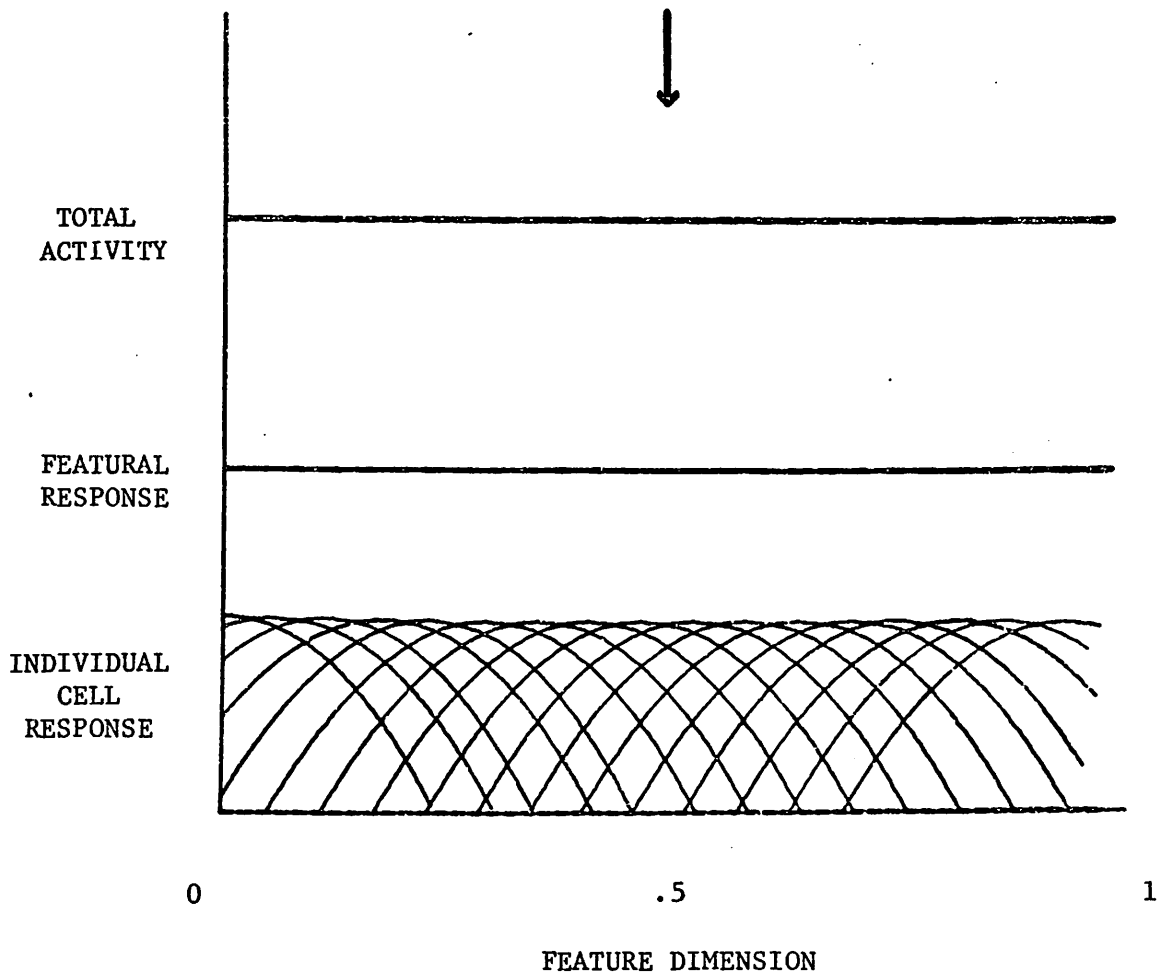


Figure 2.1 A uniform distribution of response curves, spaced evenly throughout a feature dimension, with equal tuning widths, $\omega = .5$.

shunting inhibition of pre- and post-synaptic cell layers (Grossberg, 1973). (See von der Malsburg, 1973, Figures 7, 8, and 9 for a demonstration of these changes.) The position, x_i , of the tuning curve shifts toward the input, v :

$$\tau_x \dot{x}_i(t) = -x_i(t) + f_i + \Delta_x [v - f_i] a_i(v). \quad (2.3)$$

The tuning width, ω_i , narrows:

$$\tau_\omega \dot{\omega}_i(t) = -\omega_i(t) + \omega_0 - \Delta_\omega a_i(v). \quad (2.4)$$

The peak output activity, h_i , grows:

$$\tau_h \dot{h}_i(t) = -h_i(t) + h_0 + \Delta_h a_i(v). \quad (2.5)$$

Aside from positive synaptic modification a fourth way tuning curves can be modified by experience is by threshold elevation:

$$\tau_\theta \dot{\theta}_i(t) = -\theta_i(t) + \Delta_\theta a_i(v) \quad (2.6)$$

but it is assumed on the basis of discussions in sections 2.1.1.-2.1.3. that the time scale of (2.6) is much shorter than that for (2.3) - (2.5). All changes in the parameters of the tuning curve of a cell are driven by cell activity, a_i .

To study the effects of modification of $\{a_i\}$ by an input, v , on the featural response, R , a computer simulation was undertaken. An initial distribution could be defined as in Figure 2.1 by specifying ω , h and θ were initially set to 1 and 0 respectively. Any of the four types of modification could be applied in any combination by specifying Δ_x , Δ_ω , Δ_h , Δ_θ , and a modifying stimulus, v_m . Modification was applied once and any of four output graphs could be dis-

played. All graphs are plotted over the same abscissa $v \in [0,1]$ but displaced and scaled vertically. The total activity of the distribution is defined as:

$$A(v) = \sum_i a_i(v). \quad (2.7)$$

The featural response measure, $R(v)$ defined in (2.2), is plotted as the deviation from v for easy comparison. A subset of $\{a_i\}$ is plotted to show how v_m affects individual response curves. The thresholds are represented by a dotted line plotted on the same ordinate as the individual response curves.

Figures 2.2 through 2.5 show the effects that each of the four types of plasticity alone have on the output. (2.3) and (2.5) alone have positive aftereffects near v_m . (2.4) and (2.6) have negative aftereffects. The right balance of (2.3), (2.4), and (2.5), which are the types of changes demonstrated by the Malsburg model, produce negative aftereffects (Figure 2.6). Note that positive aftereffects in Figure 2.2 can have negative aftereffects further away from v_m . This is the key point of the ME model in Chapter III. Negative aftereffects at white have little to do with the effects at the adaptation input. Threshold elevation alone (Figure 2.5) can produce the same shaped response curve as positive synaptic modification (Figure 2.6) but the activity at v_m differs. With all four types of plasticity operating together (Figure 2.7) it is even possible to get a greater number of units clustered about v_m and reduced activity at v_m at the same time. Contradictory results in developmental plasticity may be partly explained by these results. If in addition to several types of plasticity effects operating in different regions of the feature

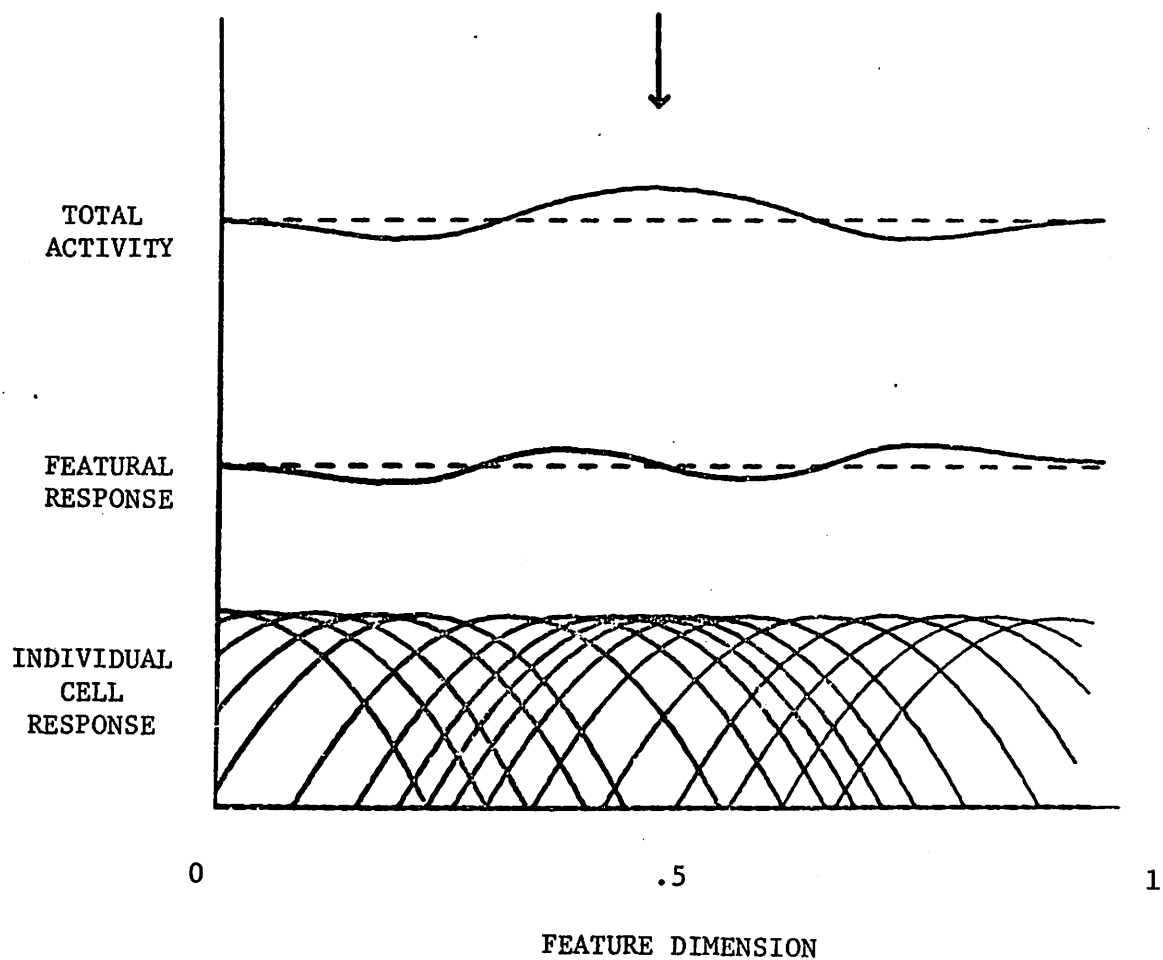


Figure 2.2 The changes in the total activity and featural response produced by shifting of individual response curves, toward the modifying stimulus. Note the slight positive, then negative featural aftereffect near v_m . $\omega = .5$, $v_m = .5$, $\Delta_x = .5$, $\Delta_\omega = \Delta_h = \Delta_\theta = 0$.

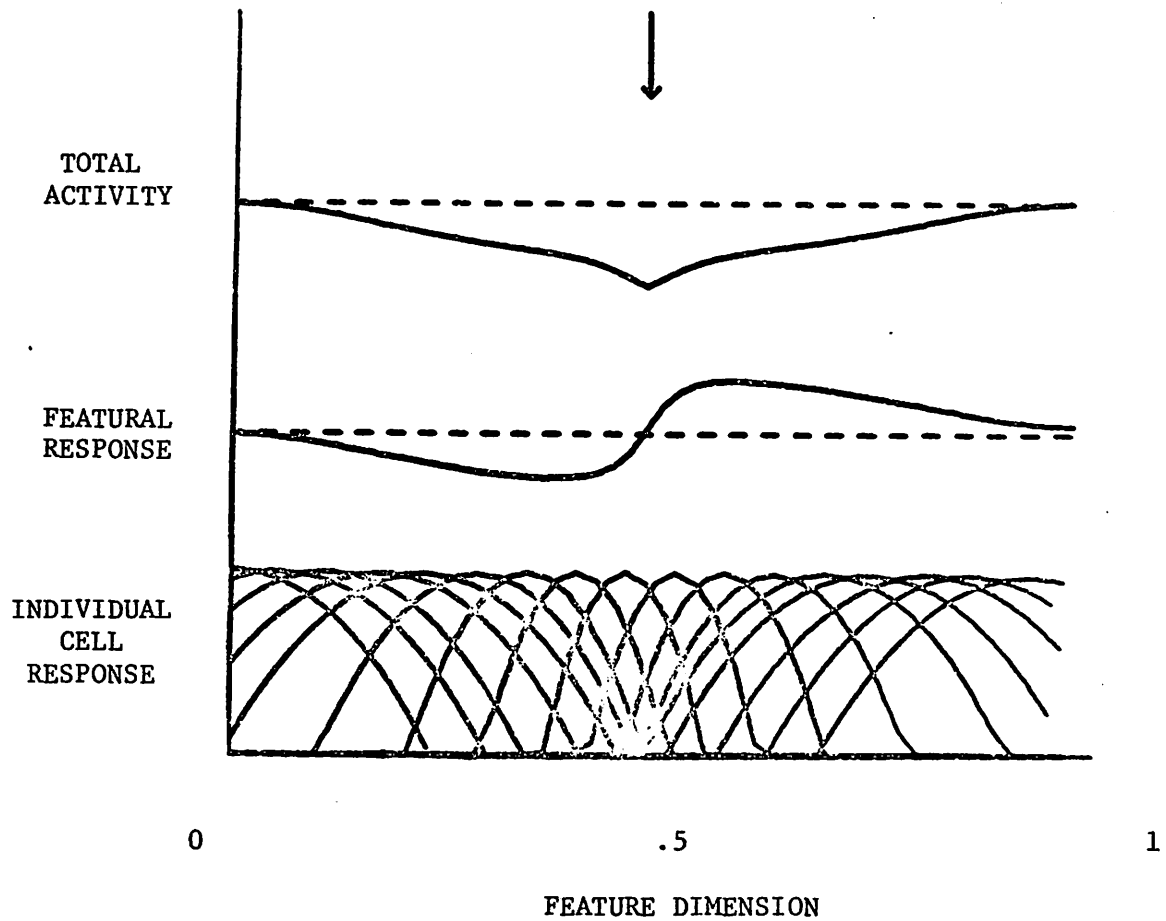


Figure 2.3 The changes in the total activity and featural response produced by decrease of individual tuning curve widths near the modifying stimulus. Note the negative after-effect near v_m . $\omega = .5$, $v_m = .5$, $\Delta_\omega = .15$, $\Delta_x = \Delta_h = \Delta_\theta = 0$.

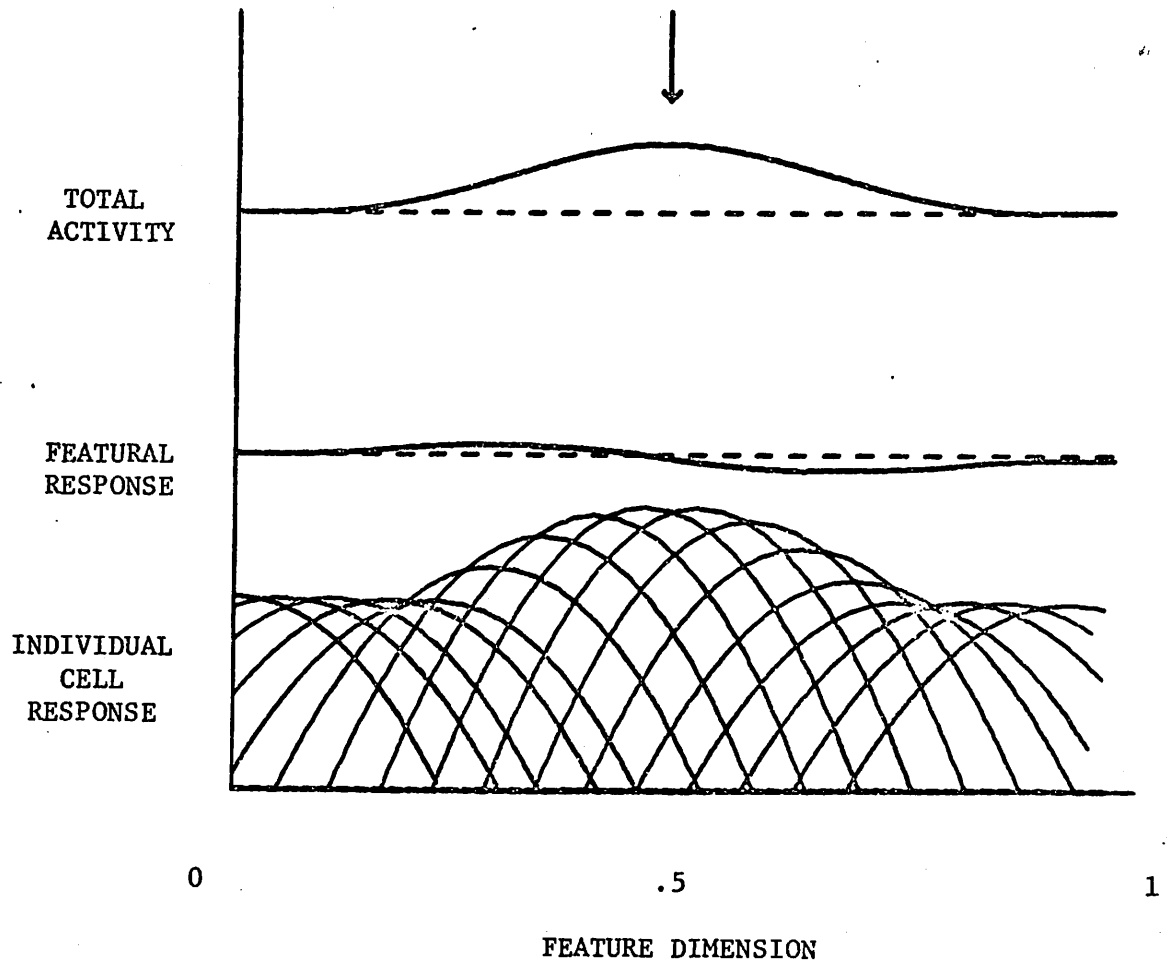


Figure 2.4 The changes in the total activity and featural response produced by increase of individual response curve heights near the modifying stimulus. Note the only slight positive aftereffect near v_m although Δ_h is quite large. $\omega = .5$, $v_m = .5$, $\Delta_h = .5$, $\Delta_x = \Delta_\omega = \Delta_\theta = 0$.

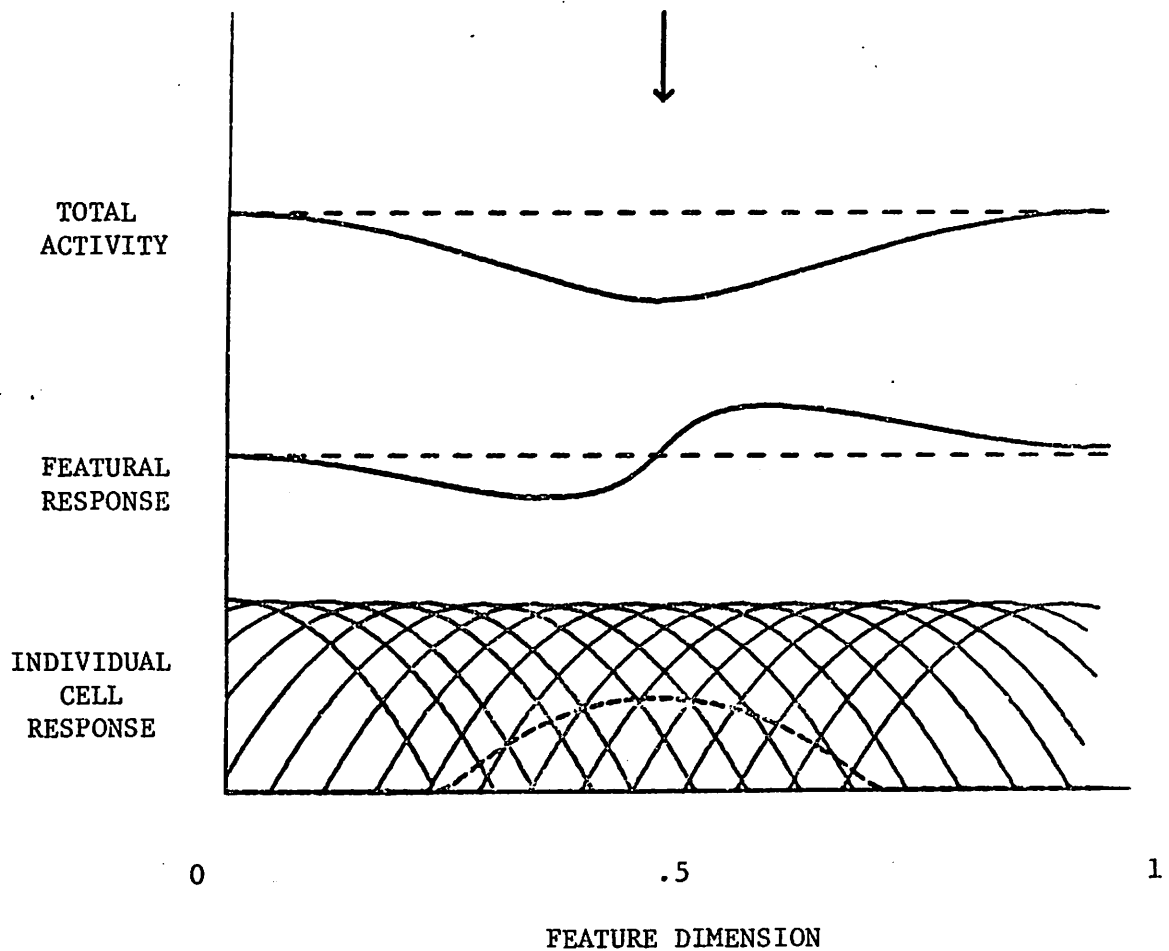


Figure 2.5 The changes in the total activity and featural response produced by increase of individual response curve thresholds near the modifying stimulus. The dotted line plotted with the response curve distribution gives the height of thresholds. Note the negative aftereffect near v_m . $\omega = .5$, $v_m = .5$, $\Delta_\theta = .5$, $\Delta_x = \Delta_\omega = \Delta_h = 0$.

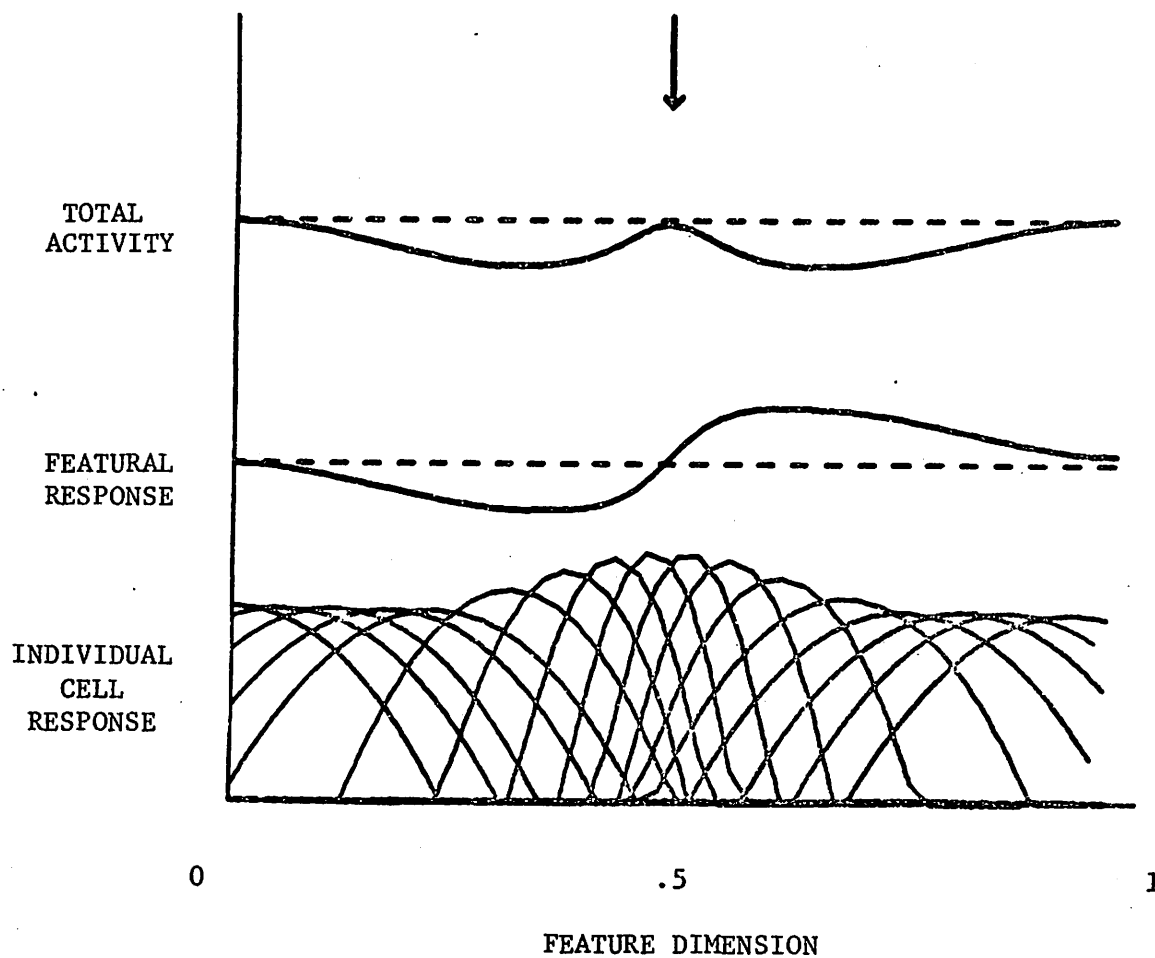


Figure 2.6 The changes in total activity and featural response produced by shifting, narrowing, and heightening of individual response curves near the modifying stimulus. Note the zero change in activity at v_m and the negative aftereffect near v_m . $\omega = .5$, $v_m = .5$, $\Delta_x = .3$, $\Delta_\omega = .15$, $\Delta_h = .3$, $\Delta_\theta = 0$.

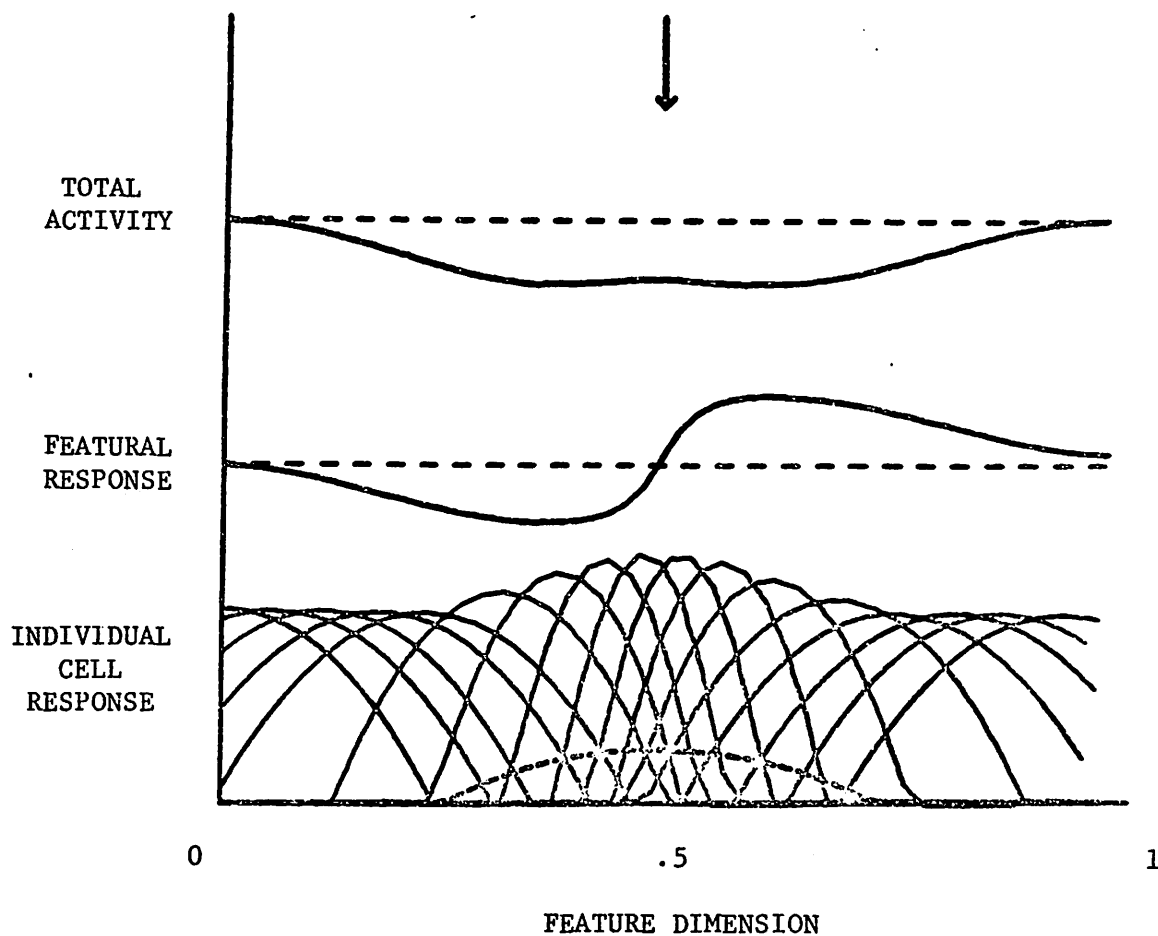


Figure 2.7 The changes in the total activity and featural response produced by shifting, narrowing, and heightening of individual response curves and increasing of thresholds near the modifying stimulus. Note the negative featural aftereffect near v_m . $\omega = .5$, $v_m = .5$, $\Delta_x = .3$, $\Delta_\omega = .15$, $\Delta_h = .3$, $\Delta_\theta = .3$.

scale in different directions, there exist different time constants for synaptic plasticity versus threshold elevation, interpretation of the experimental results is even more confounded. But recognition of the various types of plasticity in both developmental studies and adaptation studies can lead to a unification of both fields. The tilt aftereffect, spatial frequency aftereffects, motion aftereffects, and the McCollough effect can all be explained by synaptic modification as illustrated in Figure 2.6. Note the similarity between this figure and Blakemore and Sutton's (1969) Figure 2. Note the similarity between Figure 2.8 and the tilt aftereffect curve in Figure 5 of Morant and Harris (1965).

Two aspects of the tilt aftereffect are not explained by a uniform distribution of simple unconnected elements: adaptation and the indirect effect.

Adaptation can be explained by an inhomogeneity in the distribution of orientation detectors. If there are more units clustered at vertical and horizontal than at oblique angles, adaptation near the vertical will draw more vertical units toward v_m than oblique units. The response at v_m during inspection will become progressively biased toward vertical because the rise in the density of detectors on the vertical side will be unmatched by the sparser density on the oblique side. There is some evidence for a greater density of orientation detectors at vertical and horizontal in the foveal part of the visual field in rhesus monkeys (Mansfield, 1974).

The indirect effect is an apparent tilt induced in lines greater than 45° away from an adaptation stimulus. Inspection of a line tilted less than 45° clockwise from vertical induces an apparent

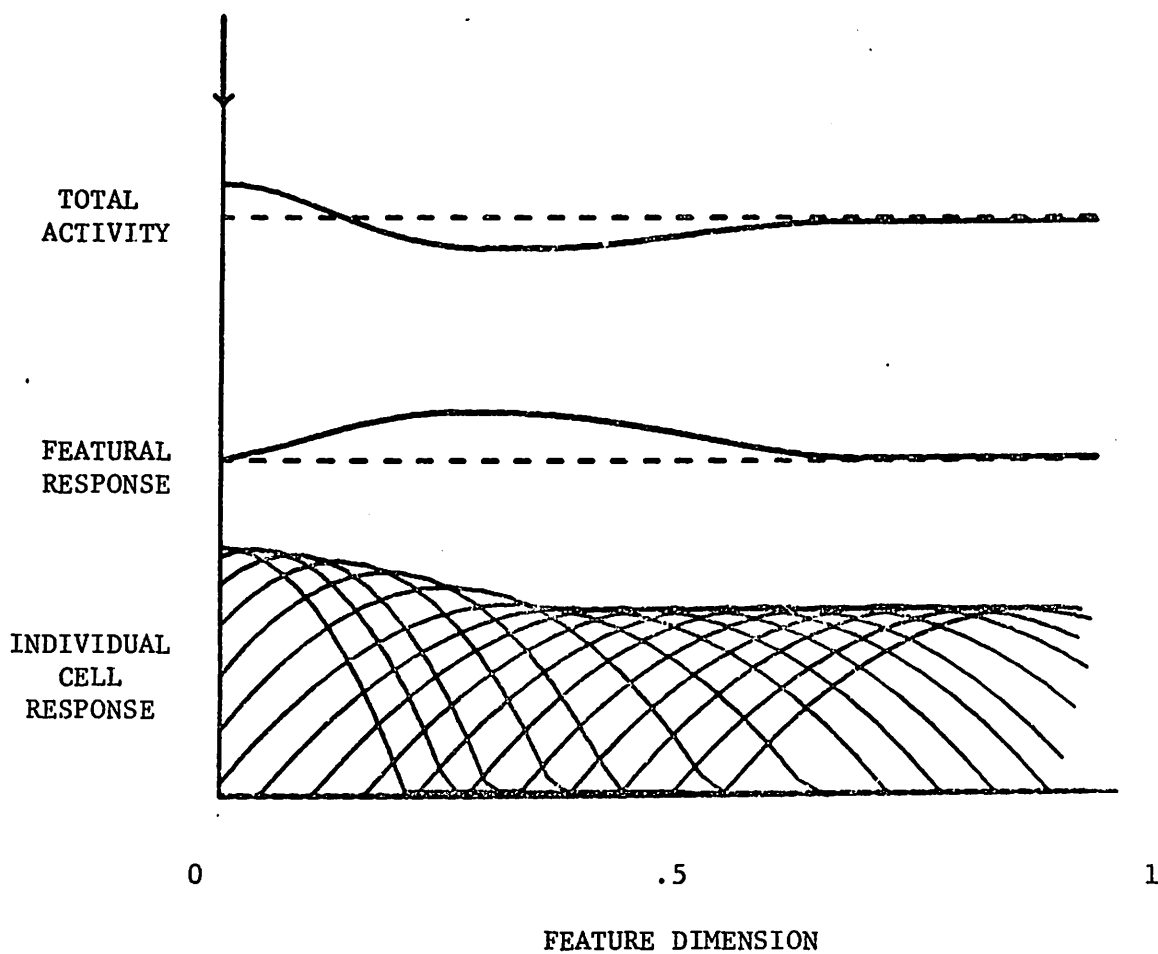


Figure 2.8 The changes in the total activity and featural response produced by shifting, narrowing, and heightening of individual response curves near the modifying stimulus. $\omega = .75$, $v_m = 0$, $\Delta_x = .3$, $\Delta_\omega = .15$, $\Delta_h = .3$, $\Delta_\theta = 0$.

counterclockwise tilt in an objectively horizontal line (indirect effect). Although simulation is necessary to substantiate the claim, it is possible that inhibitory coupling of units having orthogonal responses to orientation could produce a change in the right direction 90° away from the inspection figure. A change in the response curve at an angle, θ , would induce a change in the response at $\theta \pm 90^\circ$ through inhibitory connections. It is not intuitively clear in which direction the indirect effect would occur given this hypothesis. Further simulation is necessary. Inhibitory coupling of orthogonal line detectors is indicated by the image processing work of Zucker, Hummel, and Rosenfeld (1975).

2.2. Applications in Image Processing

What is plasticity in the visual system good for? Does it have anything to do with computations necessary for "seeing?" A brief look at some of the techniques in computer vision reveals a striking similarity between biological visual plasticity and computer feature extraction techniques. The comparisons are highly speculative. They are meant merely as pointers to the hazy area where brain theory and computer vision may one day meet. The mathematical development is still missing, but it is my belief that rubbing together concepts in both fields is necessary to an understanding of vision abstracted from details of the implementation in either computers or brains.

The von der Malsburg (1973) network appears to be doing feature extraction in one primitive feature dimension: line orientation. The same technique extended to more than one dimension is reminiscent of clustering in primitive feature space. At the other extreme, long-

lasting aftereffects and adaptation are reminiscent of histogram transformation. Methods of feature extraction and scaling are crucial to segmentation of a complex, noisy scene into meaningful regions.

2.2.1. Segmentation

Segmentation is the process of separating a scene into regions to be interpreted by a higher level process, pieced together and labeled as objects. A region's subparts coalesce by virtue of uniformities of a property measured everywhere in the scene. The best way to pick properties and to scale measures of properties is related to feature tuning and clustering. The idea is to choose a measure that is relatively constant within objects and changes abruptly across object boundaries. The choice is, in general, scene dependent. Tuning and clustering will be discussed in the next two sections.

In pattern recognition the property typically chosen for segmentation is luminance, but more complex, natural or noisy scenes require more complex properties such as classes of texture measures, color measures, color-texture measures, texture-orientation and line-orientation measures. A particularly powerful technique for segmentation is the use of iterative networks that represent the input with multiple feature measures at each location in the scene (however coarsely it is partitioned). Through iteration the network reaches an equilibrium in which regions are represented as patches of high activity at different layers in the network. Contiguous units signaling the same values of a property enhance each other while units signaling different values suppress each other (Montalvo, 1975; Amari and

Arbib, 1976). Mutual enhancement or suppression is carried out through nonlinear excitatory and inhibitory feedback. Two examples of this type of network are a line/region detection network by Zucker, Hummel, and Rosenfeld (1975) and a stereopsis network by Dev (1975). Contiguity in space biases a unit's estimate of a property toward its neighbor's estimate. In this way patches of contiguous units become associated if their estimates are similar. Similarity is defined by the function through which connected units influence each other.

Segmentation in iterative interconnected networks is a way of dynamically defining or scaling property measures through local interactions. Grossberg (1975) shows how short-term activity, if it persists long enough through prolonged stimulation, can become coded into synapses. Whatever distortions may have been present in the activity may be reflected in the long-term storage also. Segmentation networks are designed to enhance contrast across the feature dimension. If a prolonged stimulus at one feature value produces contrast enhancement for a long period of time, the distortion may be coded into long-term memory by the synapses. Long lasting negative aftereffects may just be the result of short-term contrast enhancement being coded into synapses by the presense of prolonged stimulation by the same feature.

Segmentation networks actually make use of this contrast enhancement in order to define regions dynamically based on local properties of the input scene.

2.2.2. Tuning

Tunability of a range of feature detectors is related to histogram transformation (Hummel, 1975) in image processing. Histogram uniformization is a transformation of the set of quantization levels of a property measure of the picture points so that an equal number of picture elements will fall into each bin. Uniformization is typically applied to gray level histograms to increase contrast. It has also been applied to measures of texture (Rosenfeld and Troy, 1970). When a non-uniform histogram, $g(v)$, plotted along some feature dimension, v , is transformed into a uniform histogram, $k(z)$, the information content of the new quantization is maximized (Hummel, 1975). (See Figure 2.9.) The model for tunable feature space discussed in section 2.1.4. can approximate the process of histogram uniformization given certain constraints on the tuning curve parameters. Suppose that heights are constant, widths are inversely proportional to the smoothed input distribution, $\bar{g}(v)$, and the spacing between curves is inversely proportional to $\bar{g}(v)$:

$$h_i = 1,$$

$$\omega_i = \frac{\omega_0}{\bar{g}(x_i)},$$

and

$$x_i - x_{i-1} = \frac{f_i - f_{i-1}}{\bar{g}(v)}$$

where

$$\bar{g}(v) = \int_{v-\omega_0}^{v+\omega_0} \left[1 - \left(\frac{u-v}{\omega_0} \right)^2 \right] g(u) du. \quad (2.8)$$

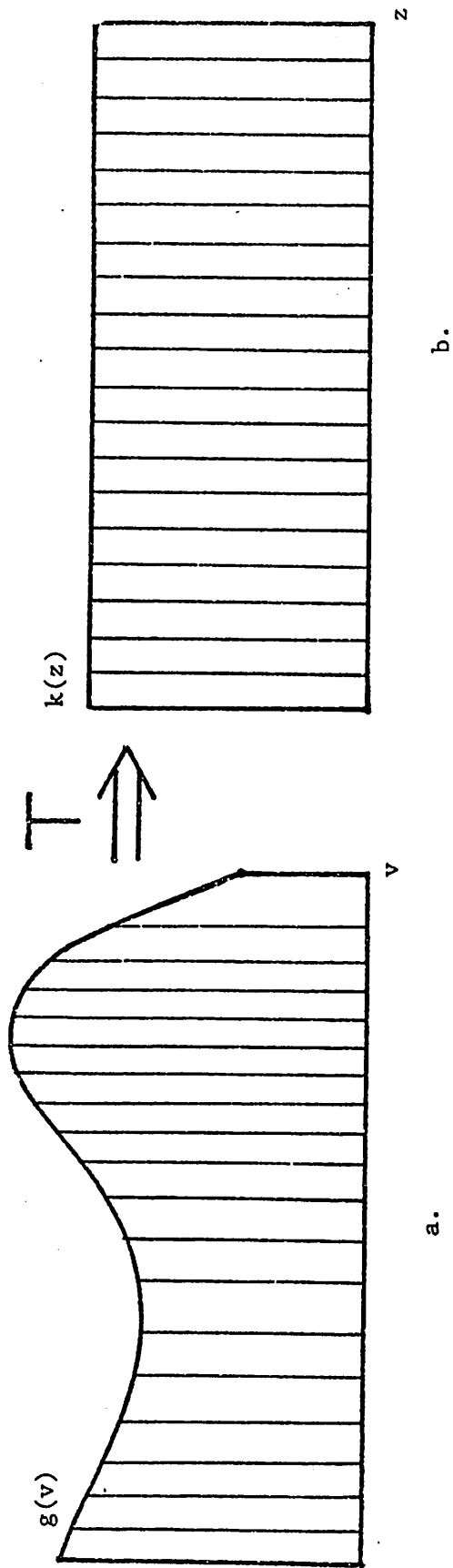


Figure 2.9 Histogram uniformization. The number of picture points, $g(v)$, plotted against the physical feature scale, v , is equalized by a transformed quantization, z , that keeps the area in each bin constant.

If $\bar{g}(x_i) - \bar{g}(x_{i-1})$ is small for all $i=1,2,\dots,n$ and $\omega_0 n$ is small, then the activity of the network, $A(v)$, will be about constant (see Appendix A). The number of inputs coded by each detector will also be about constant:

$$\begin{aligned}
 k(f_i) &= \int_{x_i - \omega_i}^{x_i + \omega_i} a_i(u) g(u) du, & \text{with } f_i &= \frac{i}{n} \\
 &\approx \bar{g}(x_i) \int_{x_i - \omega_i}^{x_i + \omega_i} a_i(u) du \\
 &= \bar{g}(x_i) \frac{4}{3} \omega_i = \frac{4}{3} \omega_0. & (2.9)
 \end{aligned}$$

The transformation of the input distribution, $g(v)$, to an internal feature space distribution, $k(f_i)$, is illustrated by Figure 2.9.

The discriminability of the set of detectors $\{D_i\}$ is inversely related to the JND (just noticeable difference). The JND is the amount of change in the input, v , needed for a noticeable (unit) change in the response, R :

$$\text{JND} = \frac{\Delta}{R(v + \Delta) - R(v)} \approx \frac{dv}{dR(v)}. \quad (2.10)$$

Thus, we can define discriminability as roughly equal to the derivative of R over v . If we do this we see that negative aftereffects increase discriminability in the neighborhood of the modifying stimulus, v_m . Whenever negative aftereffects occur (Figures 2.3, 2.5 - 2.8) the derivative of $R(v)-v$ at v_m is positive. This implies that $\frac{dR(v)}{dv} > 1$. Conversely, whenever positive aftereffects occur $\frac{dR(v)}{dv} < 1$. Given the constraints (2.8) on the set of detectors, the discriminability approximates the input distribution (see Appendix A):

$$\frac{dR(v)}{dv} \cong \bar{g}(v). \quad (2.11)$$

Thus, synaptic modification producing negative aftereffects can equalize discriminability over $g(v)$ provided modification produces a set of tuning curves with parameters specified by (2.8). The transformation is analogous to histogram uniformization that maximizes the information content of the quantization.

2.2.3. Clustering

Clustering for adaptive feature extraction is another form of histogram transformation, but in a sense, opposite to histogram uniformization. Usually an n -dimensional space (histogram), rather than a one-dimensional histogram, is partitioned on the basis of high density regions. The simplest example, in one dimension, is thresholding. In the restricted domain of white blood cell detection the gray level histogram is normally bimodal. The nucleus is segregated from the cytoplasm by dividing the gray level histogram at the lowest point between the two maxima (Figure 2.10). The nucleus is usually much darker than the cytoplasm. The old gray level scale which originally had N values is converted to a new scale containing only two values, $\{0,1\}$. One value is assigned to the cytoplasm cluster and one to the nucleus cluster. This reduces the information in the picture and separates the nucleus from the cytoplasm. The same technique can be extended to n -dimensions in order to find naturally occurring associations between primitive features (Hanson, Riseman, and Nagin, 1975). Primitive features are lumped into properties. The process is the opposite of histogram uniformization in that it minimizes information

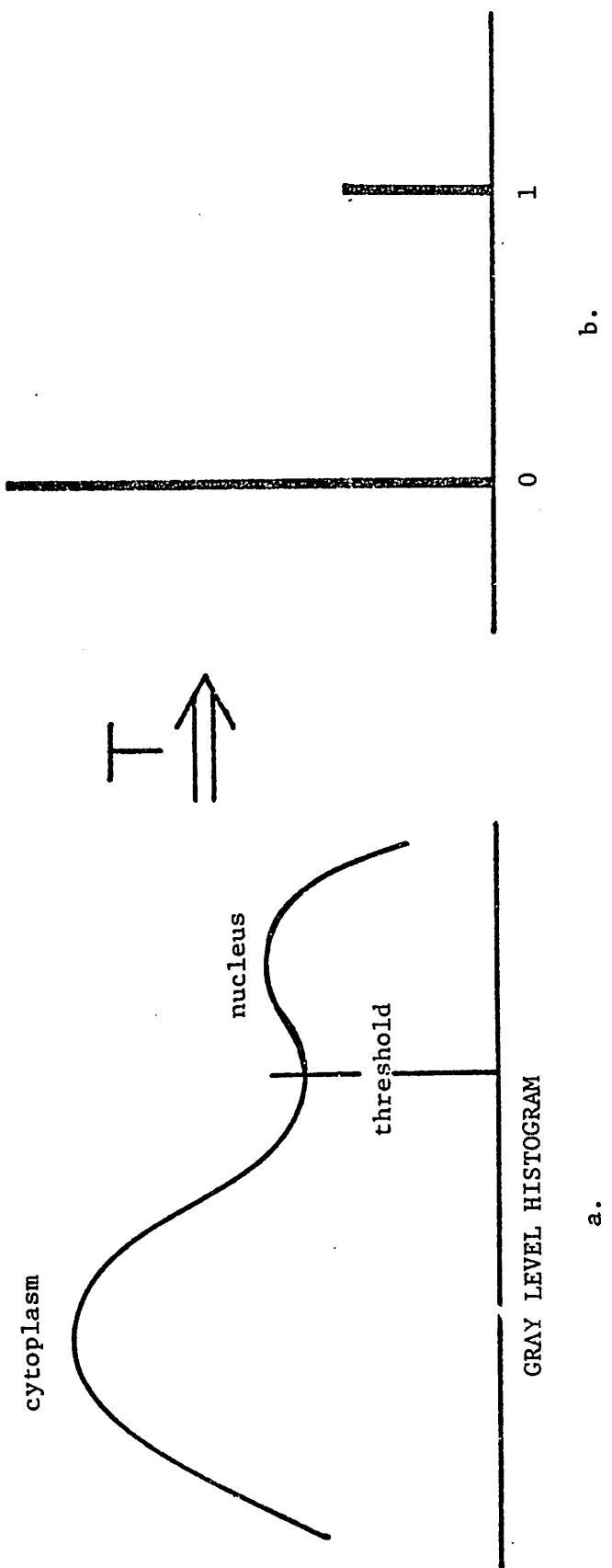


Figure 2.10 Clustering. The histogram of the number of points in the picture of a blood cell is thresholded to reduce the number of gray level values to two: 0 and 1.

rather than maximizing it. In clustering, regions of high density are lumped into one property rather than partitioned into finer gradations. The process identifies the types of complex features present in the scene.

The same type of clustering may occur in iterative segmentation networks through cooperative processes of the type that associate like feature elements across space. Nonlinear cooperative enhancement can be built up among primitive feature sets that occur concurrently over wide regions of space. Combinations of features that have a low rate of occurrence could be suppressed by neighboring configurations that differed. My current efforts are directed toward building a network model for dynamic complex-feature construction for the purpose of segmentation.

For such a model it is assumed that the number of primitive feature dimensions--color, line size, edge size, orientation, direction of movement, and disparity--is small. These are the features that have been found in single cells. For natural textures the number of operators needed to distinguish between them is on the order of six (Zorbist and Thompson, 1975). Julesz (1975) has shown that texture discrimination is based on only first and second order statistics of luminance. Higher order differences cannot be perceived by humans. Marr's (1975) analysis of texture demonstrates how first order statistics of the outputs of line (bar) size, edge size, and orientation operators are equivalent to the second order statistical operations needed to distinguish a variety of textures.

A dynamic complex-feature constructing network would use features coded by single cells as primitives, and associations through synapses

as properties for segmentation. Many primitive features, however, are often found together in single cells, such as color, orientation and size, or orientation, size and directionality of movement, or orientation, size and disparity. The problem faced by a clustering network is whether enough random variation in feature-coding cells and enough numbers of cells exist to represent the entire primitive-feature n-space at all times, or whether regions in the n-space are coded up dynamically through associating synapses whenever large regions of complex-features occur in the input. The latter seems more efficient in terms of computer vision but the physiology may be doing the former.

Perhaps contingent aftereffects (CAE) will provide a clue when the effect is isolated neurophysiologically. CAE's may be the result of short-term feature associations that have become coded into synapses by prolonged exposure, or the result of differential tuning of two different feature dimensions that coexist in the same cells. (Single-cell models and multiple-cell models will be discussed in Section 4.1.) So far CAE's have been demonstrated only for features that can coexist in single cells. Attempts to associate features that have not been found together in single cells have, up to now, failed (Favreau, 1976). In either case, however, the computational result is the association of primitive features across dimensions, analogous to clustering in image processing.

CHAPTER III

SIMULATION OF THE McCOLLOUGH-MALSBURG MODEL (MMM)

A computer simulation of the McCollough effect was conducted using a model similar to von der Malsburg's (1973) but with red and green cells at the input layer not just white-sensitive cells. This model shares many of the characteristics of Grossberg's (1976) formalization of neural networks: learning at cross-correlated synapses and on-center, off-surround interactions that attenuate cortical feedback and contrast enhance patterns of cortical activity.

3.1. von der Malsburg's Model

von der Malsburg's model consists of 19 input cells each connected to 169 excitatory cortical cells. Each excitatory cortical cell connects to its 6 nearest neighbors in a hexagonal array, to the corresponding 6 cells in a 169-cell inhibitory layer (I), and to the I-cell corresponding to itself. Each I-cell in turn connects to a 12-cell surround in the excitatory layer (E). (See Figure 3.1.) Cells compute a weighted sum of their inputs from all layers, subtract a threshold, and output the result if it is positive and zero otherwise. The postsynaptic potential of each cell at each iteration is calculated by:

$$E'_k = aE_k + \sum_{i=1}^{19} s_{ik} R_i^* + \sum_{i=1}^6 C_{EE} E_i^* - \sum_{i=1}^{12} C_{IE} I_i^* \quad (3.1)$$

for excitors and

$$I'_k = bI_k + \sum_{i=1}^7 C_{EI} E_i^* + C_I \quad (3.2)$$

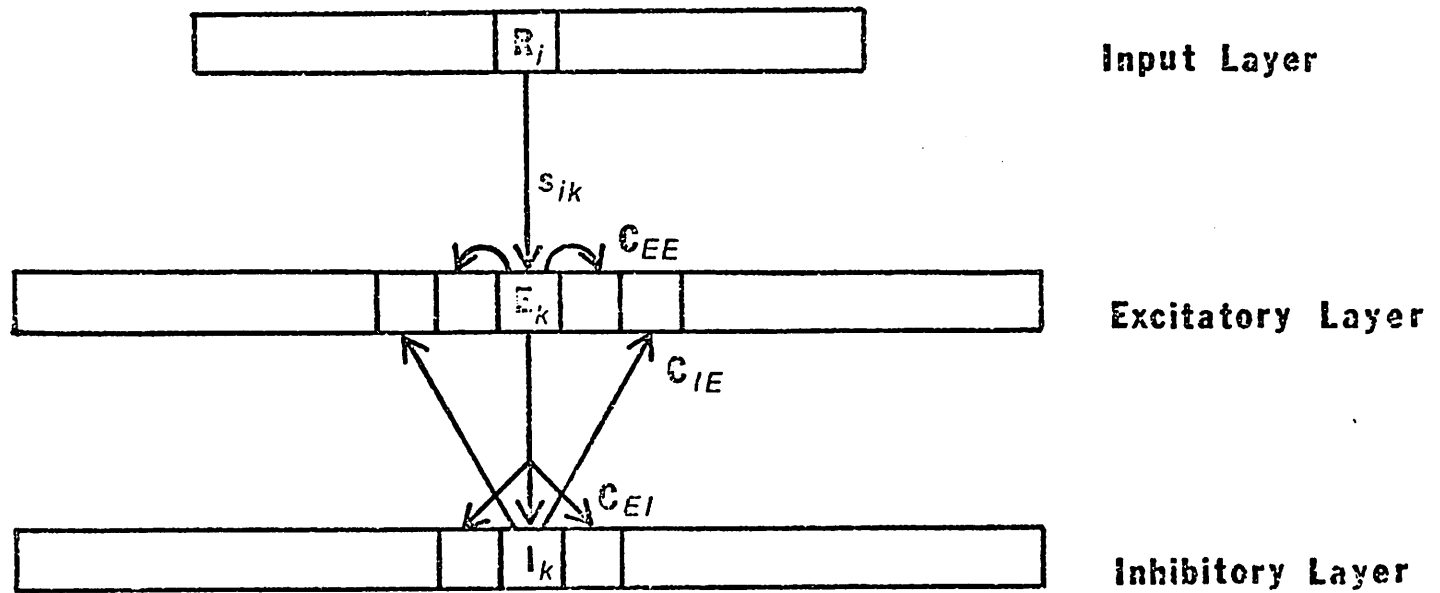


Figure 3.1 Side view of hexagonal input and cortical arrays showing the connectivity between and within the layers. The C's represent constant connection strengths within E and I layers and the s_{ik} 's represent modifiable synapses between R and E layers.

for inhibitors, where a and b are decay constants for each iteration, s_{ik} is the synaptic weight from input cell R_i to cell E_k , C_I is a constant input to I and C_{AB} is the synaptic weight constant from a cell in layer A to one in layer B. A synapse s_{ik} is modified when R_i and E_k fire simultaneously according to the rule:

$$s'_{ik} = s_{ik} + \Delta R_i^* E_k^* \quad (3.3)$$

where s'_{ik} is the new value, s_{ik} is the old, Δ is the learning constant, and $*$ is the thresholding function:

$$x^* = \begin{cases} x - \theta & \text{if } x > \theta \\ 0 & \text{if } x \leq \theta. \end{cases} \quad (3.4)$$

θ is the threshold. The sum of each cortical cell's input synapses is held constant at C_s by renormalization after the modification step:

$$s_{ik} = s'_{ik} \frac{C_s}{\sum_{i=1}^{19} s'_{ik}} \quad (3.5)$$

The input stimulus set consists of 9 lines at different orientations, each line stimulating 7 input layer (R) units. (See von der Malsburg, 1973 for further details.)

3.2. A Color Version of Malsburg

The McCollough-Malsburg-Model (MMM) is a color version of von der Malsburg's self-organizing model of cortex. The major change is that MMM's input layer "sees" red and green in addition to black and white. Instead of having achromatic on-cells in the input layer MMM

has a red on-cell and a green on-cell for every achromatic R-cell in the von der Malsburg model. Thus, there are a total of 38 R-cells connected to 169 excitatory cortical cells. The spatial arrangement of R is identical to von der Malsburg's except that each input position contains a red and green cell in the same location.¹

The stimulus set for MMM varies not just in orientation but in the amount of red/green saturation. The variable v represents a point on a saturation continuum from pure green through white to pure red of equal luminance. Some care was necessary in choosing a function of v to represent color that would allow E-cells to be tuned to a continuous range of v rather than just two values: red ($v = 1$) and green ($v = 0$). The need for this will become clear in the discussion section.

3.2.1. Some Initial Attempts at Color Coding

Let w_1 and w_2 be the synaptic weights associated with the green and red cells at one input location, respectively. The first function tried is the most obvious:

$$f_o(v) = w_1(1 - v) + w_2(v). \quad (3.6)$$

¹ The input layer in MMM corresponds to von der Malsburg's retinal layer. The red and green cells in MMM do not necessarily represent red or green cone cells. They can represent any color-specific ganglion, lateral geniculate or cortical cells located before the cortical layers E and I modelled here.

Since f_0 is a linear function of v there can be only two possible maxima over $v \in [0,1]$ for fixed synaptic pairs (w_1, w_2) . These maxima are at $v = 0$ or at $v = 1$. Using f_0 as input an E-cell can fire maximally only to pure red or pure green.

A second function tried,

$$f_1(v) = w_1[1 - kv^2]^+ + w_2[1 - k(v - 1)^2]^+ \quad (3.7)$$

where $+$ is the threshold function with $\theta = 0$, is based on the general shape of red and green opponent-color cells in LGN over wavelength (Figure 3.2), disregarding the inhibitory component (DeValois, Abramov, and Jacobs, 1966). The trouble with this formulation for color is that it does not allow tuning to a specific combination of red and green either. To illustrate this point let us suppose that E-cells have only two inputs with weights w_1 and w_2 . Also suppose that $w_1 + w_2 = C$ for all cells and that v is fixed at some $v_0 \in (0, .5)$. We wish to train the best responders to v_0 such that they will fire maximally to v_0 . The best responders to v_0 are those with $w_1 = C$ and $w_2 = 0$. But these cells fire even more strongly to $v = 0$. So differential training to v_0 cannot occur, only to $v = 0$ or $v = 1$.

3.2.2. f_2 Version

The third color coding function tried,

$$f_2(v) = (w_1 + w_2) \left[1 - k \left(v - \frac{w_2}{w_1 + w_2} \right)^2 \right]^+ \quad v \in [0,1] \quad (3.8)$$

has the same general shape as opponent-color cells' response in LGN but also has the additional property that for a given v_0 the maximum

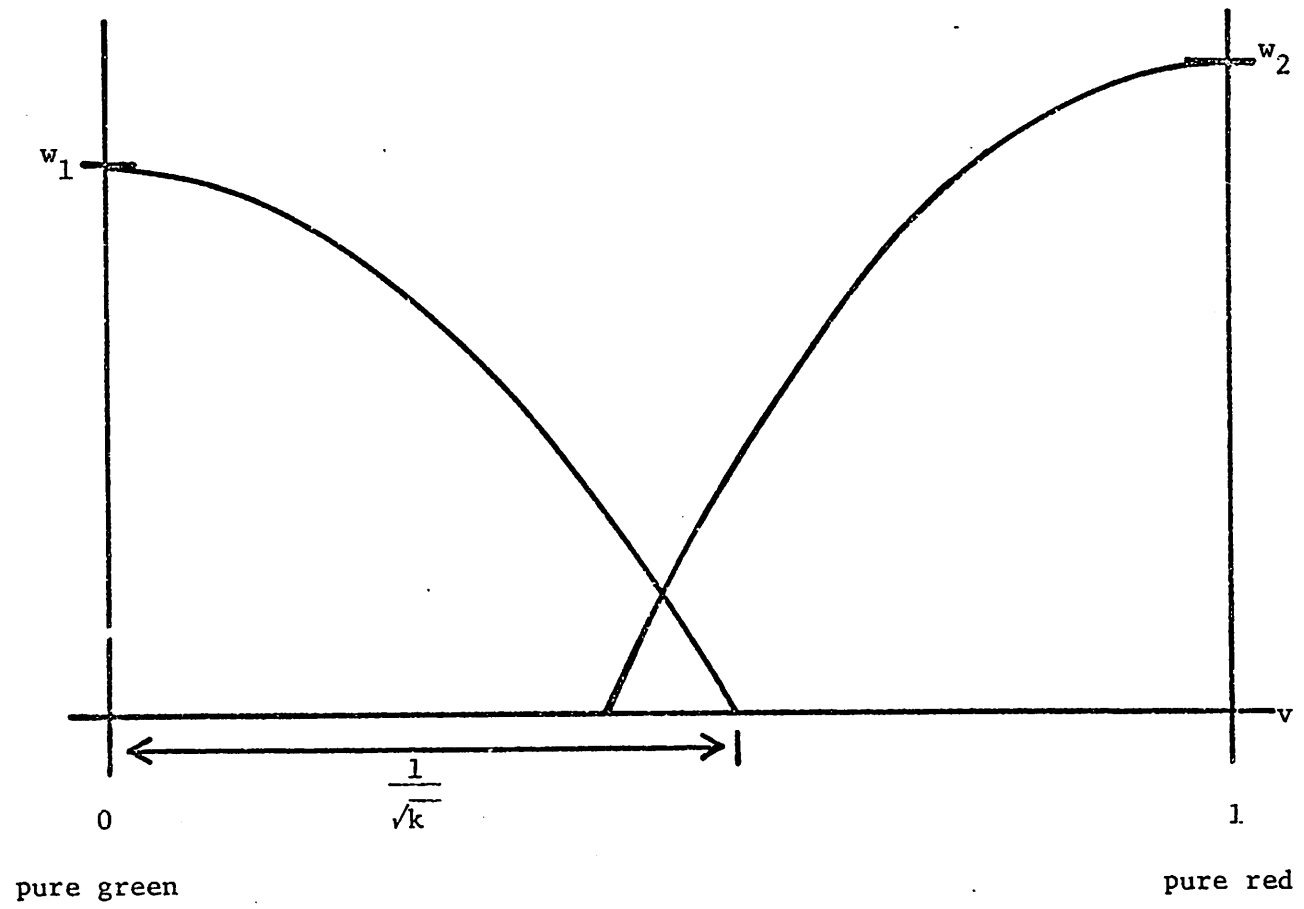


Figure 3.2 Weighted input from red and green opponent-color cells corresponding to color coding function f_1 .

responders for a constant (w_1, w_2) are those with $w_2/(w_1 + w_2) = v_0$, a specific synaptic pair ratio reflecting v_0 . This is the necessary property for specific tuning to v_0 . k is a tuning-width parameter. (See Figure 3.3.)

In all of the following versions of MMM the amount of inhibition was 5 times that in von der Malsburg's network so that fewer cells would go on to each stimulus. This was necessary in order for cortical cells to differentiate stimuli over two dimensions not just line orientation. In addition to this, the excitatory and inhibitory thresholds in the f_2 version vary according to the average synaptically weighted input to E-cells. (See Table 3.1.) In the original model the average input to cortical cells was approximately constant over all stimuli, with only slight variations due to randomly assigned synaptic weights. In this version red and green synaptic weights were assigned independently from a uniform distribution over the interval $[0, .1]$. This induced an initial distribution of cortical cells with peak responses clustered at $v = .5$ (Figure 3.4a). Thus the level of firing of the naive network was greatest for $v = .5$ and very low for $v = 0$ or 1 .

In order to insure uniform training to all stimuli the total firing of the network must be about constant over stimuli, otherwise the resulting distribution of units after training will not approximate the input distribution. So in order to keep the level of firing and the number of cells on approximately constant, a variable threshold was used for E and I layers in addition to a variable input to I. The variable threshold approximates a normalized input.

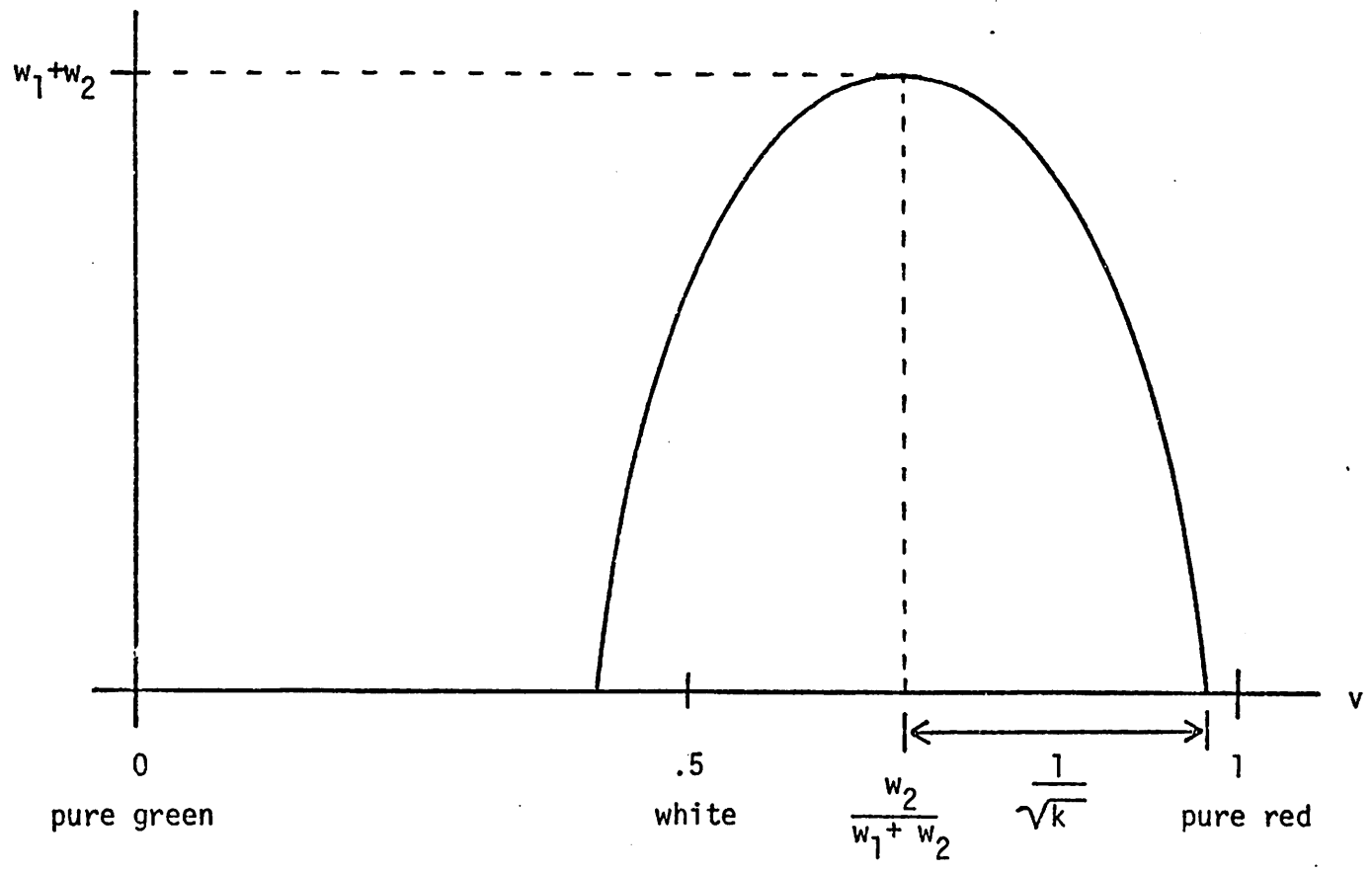


Figure 3.3 Red/green synaptic pair response to saturation, v , corresponding to color coding function f_2 .

PARAMETERS CONSTANT OVER ALL RUNS.

a	.6	E-cell decay
b	.3	I-cell decay
C _{EE}	.16	E to E-cell weight
C _{EI}	1.0	E to I-cell weight
C _{IE}	.6	I to E-cell weight
C _s	38s	sum or magnitude of synaptic weights to E-cell*

PARAMETERS AND EQUATIONS USED IN EACH RUN. EACH RUN IS REPRESENTED BY A COLUMN AND IS LISTED IN ORDER AS DISCUSSION IN THE TEXT. NUMBERS IN PARENTHESES REFER TO EQUATION NUMBERS. A DASHED ENTRY MEANS THAT THE PARAMETER OR EQUATION IS NOT APPLICABLE.

	f ₂	f ₃	f ₄	f ₄	f ₂	f _o	f _o	f _o	f _o	f _o	f _o	f _o	f _o	color coding function
C _I	\bar{E}	.4	.4	.4	.4	.4	.4	.4	.4	.4	.4	.4	.4	input to I-cell
\bar{s}	.05	.05	.0125	.0125	.05	.025	.025	.025	.025	.025	.025	.025	.025	average synaptic weight*
Δ	.05	.05	.05	.01	.01	.05	.05	.05	.05	.05	.05	.05	.05	synaptic increment
θ_E	$\bar{E}/.4+.25$	1.125	1.875	1.875	1.125	1.125	1.125	1.125	1.125	1.875	1.875	1.875	1.875	E threshold [†]
θ_I	$\bar{E}/.7+.01$.58	.58	.58	.58	.58	.58	.58	.58	.58	.58	.58	.58	I threshold
k	4.	7.1	-	-	3.	-	-	-	-	-	-	-	-	color curve width parameter
α	-	-	-	-	.28	.82	.82	.90	.95	.95	.95	.95	.95	synaptic decay
u _∞	-	-	-	-	-	-	1.	1.	1.	.5	.5	.5	.5	parameter in (3.16)
x _o	-	-	-	-	-	-	.25	.25	.25	.1	.1	.1	.1	parameter in (3.16)
g	-	-	-	-	-	-	-	-	-	-	7.	8.	10.	threshold gain
	2	8	2	10	0	2	2	2	2	2	6	4	4	# of uniform training blocks
	20	20	20	-	20	-	-	-	-	-	-	-	-	# of alternate ME presentations
	S	S	C	C	C	C	C	C	C	C	C	C	C	weights chosen uniformly over
	(3.3)	(3.3)	(3.3)	(3.3)	(3.13)	(3.14)	(3.15)	(3.15)	(3.15)	(3.15)	(3.15)	(3.15)	(3.15)	synaptic modification equation
	(3.5)	(3.5)	(3.11)	(3.11)	-	-	-	-	-	-	-	-	-	synaptic conservation equation
n	38	19	38	38	38	38	38	38	38	38	38	38	38	# of retinal units

$$\bar{E} = \frac{1}{169} \sum_{k=1}^{169} \sum_{i=1}^n s_{ik} R_i^*$$

S = synapses

C = E-cells

* If synaptic conservation is not used, this represents the initial value.

† If threshold elevation is used, this represents the initial value.

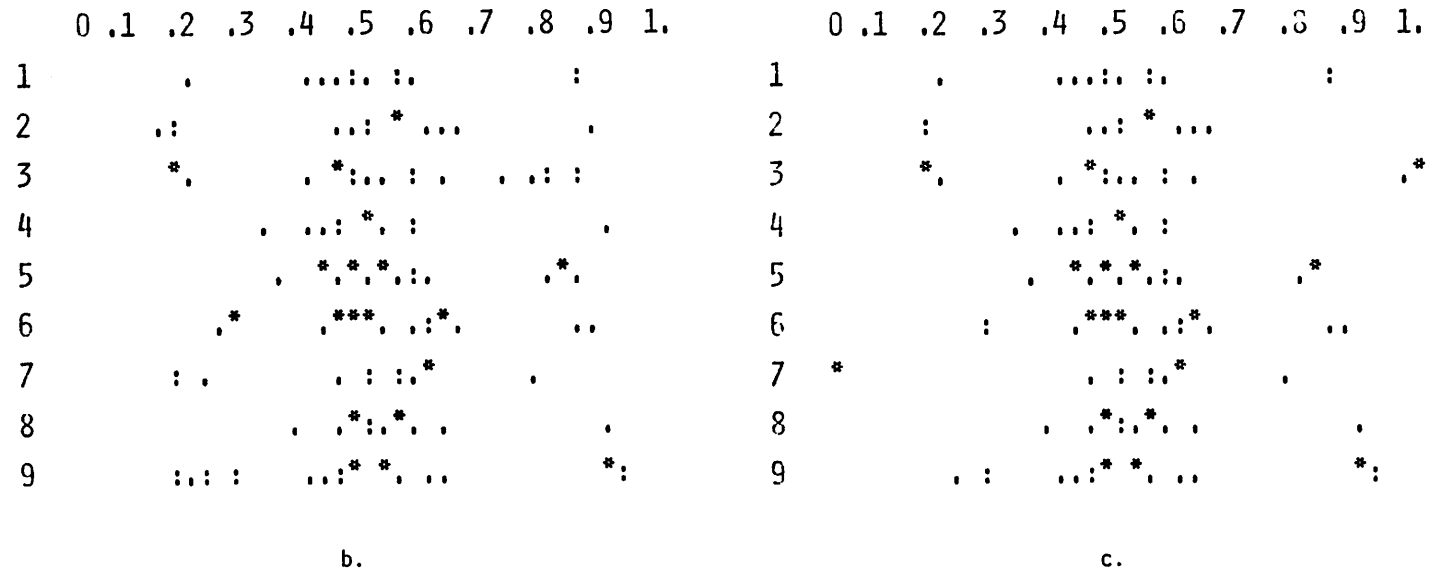
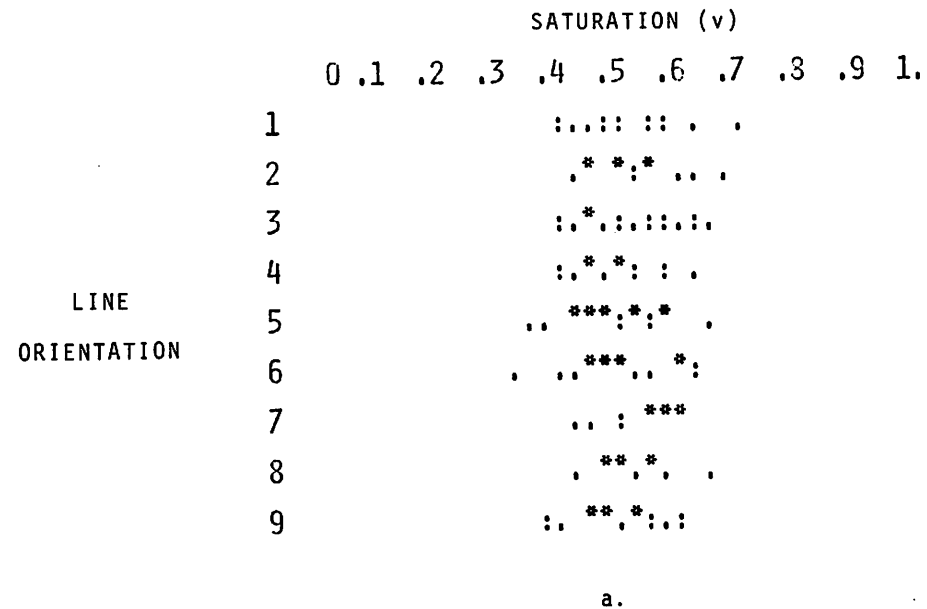


Figure 3.4 Histogram of cells plotted at their preferred saturation and orientation values using color coding function f_2 and synaptic weights assigned uniformly over synapses. Shown are (a) the initially untrained distribution, (b) the distribution after uniform training, and (c) the distribution after alternate presentations of line/color combination (3,1.) and (7,0.).

Initially all synaptic weights from layers R to E-- 38×169 of them--were randomly assigned from a uniform distribution over $[0,1]$. Synaptic modification occurred after each presentation of a randomized set of 9 line orientations (Figure 3.5) by 11 color saturation values at equal intervals within $[0,1]$. All 99 stimuli were presented twice. After each stimulus presentation the network was allowed to run to approximate equilibrium, 20 iterations, and the synapses of each E-cell that was on at this point was modified by applying (3.3) and (3.5).

After training to a uniform distribution over orientation and saturation the McCollough stimulus pair was presented alternately: line #1 with $v = 0$ followed by line #5 with $v = 1$. The synapses were modified in the same fashion after each stimulus presentation. The pair of stimuli were presented alternately 20 times.

The same ME experiment was tried on the uniformly trained network with each possible orthogonal line pair: (1,5), (2,6), (3,7), (4,8), (5,9) paired with saturation combinations (0,1) and (1,0): ten experiments in all.

The featural response of the network was calculated as follows: for every cell on after 20 iterations the cell's maximum orientation-saturation stimulus was calculated. Then the average orientation and saturation was calculated over all responding cells weighted by their degree of firing.² The response was always close to but not exactly

² The average featural response measure (2.2) as discussed in Section 2.1.4. was calculated over color and orientation, except that x_i (the new preferred stimulus) was used in place of f_i (the old label) in formula (2.2). The change does not effect the response at $v = .5$ because the cells that are activated here have not been shifted by the stimuli at the extremes. The cells that have been shifted fire little if at all to $v = .5$.

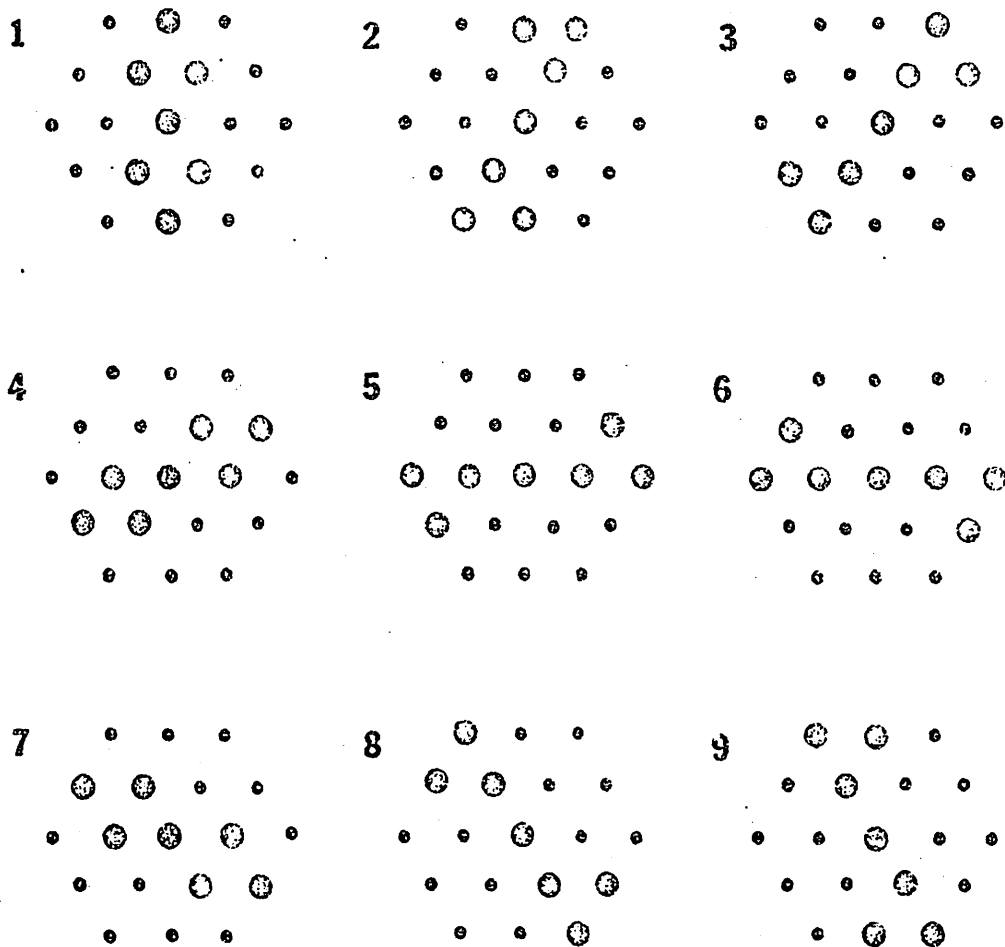


Figure 3.5 Nine line orientations presented to the input layer (R). Larger dots represent activated cells. (taken from von der Malsburg, 1973, Figure 5)

equal to the stimulus value.

Table 3.2 shows the results of ten ME experiments on the uniformly trained network. The response of the network to $v = .5$, a white line of orientation indicated, is shown before and after McCollough presentations. The difference column shows the start minus the final response. A negative increment indicates a change toward red while a positive increment indicates a change toward green. The results show that the response to a white line of a given orientation that was paired with green during adaptation changes toward pure red, while the response to an orthogonal white line paired with red changes toward pure green. The means of the differences, \bar{d}_0 and \bar{d}_1 , the standard deviations of the differences, δ_0 and δ_1 , the standard error of the mean, S_{Δ} , degrees of freedom, df , t value, and level of significance are also shown. The change in response for the two groups of cells differentially adapted is significantly different ($t = 7.007$, $df = 16$, $p < .0005$).

Figure 3.4 shows the distribution of cells plotted at the color-orientation value that produces a cell's maximum response. It illustrates the effects of 20 alternate presentations of line/color stimuli (3,1.) and (7,0.) (Figure 3.4c) on the uniformly trained network (Figure 3.4b). Units surrounding the adaptation stimuli have been shifted toward these stimuli leaving areas near $v = .5$ depleted of slightly saturated units. An input at the white test stimulus is thus biased toward the opposite color.

The preferred feature histogram does not reflect the precision of the network response, it only displays peak responses. The interactions of tuning curves give the network its fully graded output.

TABLE 3.2

The response of MFM with color coding f_2 to white test stimuli ($v = .5$) before and after alternate hue-orientation presentations. Each row represents one McCollough experiment. The adaptation and test colors (v) are specified above each block and the orthogonal line pairs are listed across rows under LINE within each block.

ADAPTATION		$v = 0$			$v = 1$			
TEST		$v = .5$			$v = .5$			
LINE	BEFORE	AFTER	d_0	LINE	BEFORE	AFTER	d_1	
1	.485	.635	-.150	5	.535	.498	.037	
2	.457	.582	-.125	6	.526	.430	.096	
3	.569	.608	-.039	7	.445	.395	.050	
4	.505	.540	-.035	8	.467	.334	.133	
5	.535	.626	-.091	9	.552	.291	.261	
[5	.535	.626	-.091]	1	.485	.405	.080	
6	.526	.694	-.168	2	.457	.418	.039	
7	.445	.623	-.178	3	.569	.413	.156	
8	.467	.603	-.136	4	.505	.472	.033	
9	.552	.662	-.110	[5	.535	.498	.037]	
		$\bar{d}_0 = -.115$				$\bar{d}_1 = .098$		
		$\delta_0 = .052$				$\delta_1 = .075$		
$S_\Delta = .0304$		$t = 7.007$	$df = 16$	$p \ll .0005$		one tailed		

* duplicate results are left out of the computation.

The histogram appears noisy because 40×9 bins are displayed, many more than the number of cells in the network. In addition, the number of training inputs (99) is comparable to the number of cells in the network (169). About 6-9 cells go on to each input--one or two for each clump of activity in the E-layer. Thus, the degree of specificity to each of the 99 inputs is not very great. Each cell has a range of about 10-15 inputs to which it will respond. Therefore, a certain degree of variability in a cell's peak response, as well as in the population response, is to be expected. The population response, however, is a much better indicator of network output than the histogram. Note that Table 3.2 more clearly demonstrates ME's than Figure 3.4c, for example.

There is a problem with the f_2 version of color coding. There is no physiological basis for a synaptic red/green pair with a response curve (3.8), and no way of arranging the interneuronal circuitry to respond according to (3.8) and change synaptic strength according to (3.3) at the same time. The synaptic behavior of f_2 is strictly a mathematically convenient color coding scheme.

3.2.3. f_3 Version

A variation of f_2 was tried in which the position of peak responses for individual red/green synaptic pairs remained stationary throughout the modification procedure. Of course, the position of a cortical cell's peak response along v could still change with variations in the synaptic strengths from different red/green pairs. Unlike f_2 , a way of realizing f_3 through interneuronal circuitry

between layers R and E is possible.

In this version there are 19 retinal positions making 169 connections to the E layer-- 169×19 in all. Each connection is randomly assigned a peak saturation-sensitivity, $m_{ik} \in [0,1]$, and weight, $s_{ik} \in [0,.1]$. m_{ik} is never modified as $w_2/(w_1 + w_2)$ was modified in f_2 . It is assumed that interneurons between R_i and E_k determine m_{ik} for each connection in the following fashion: v is the red saturation response and $1 - v$ is the green saturation response of units at R_i in the retina. These are converted to sigmoidal (Wilson and Cowan, 1973) responses dependent on m_{ik} and the tuning width parameter, k , by interneurons (Figures 3.6a and 3.6b). The outputs of this pair are multiplied before reaching E_k (Figure 3.6c). A quadratic function is used to simulate the multiplied pair of sigmoids:

$$f_3(v) = s_{ik} [1 - k(v - m_{ik})^2]^+. \quad (3.9)$$

The thresholds in the E and I layers and the input to I is held constant. (See Table 3.1.) The tuning width of (3.9) is narrower, $k = 7.1$.

Initially the network was trained to a uniform distribution over orientation and saturation by presenting eight random sequences of the same 99 input stimuli used in the f_2 version. All other procedures and parameters were the same as in the previous version.

The results of ten ME experiments on the uniformly trained network, f_3 version, are summarized in Table 3.3. Again the line orientations paired with red adaptation stimuli exhibit a green bias to white test stimuli--a positive increment--while orientations paired with green exhibit a red bias to white. The effect is weaker than

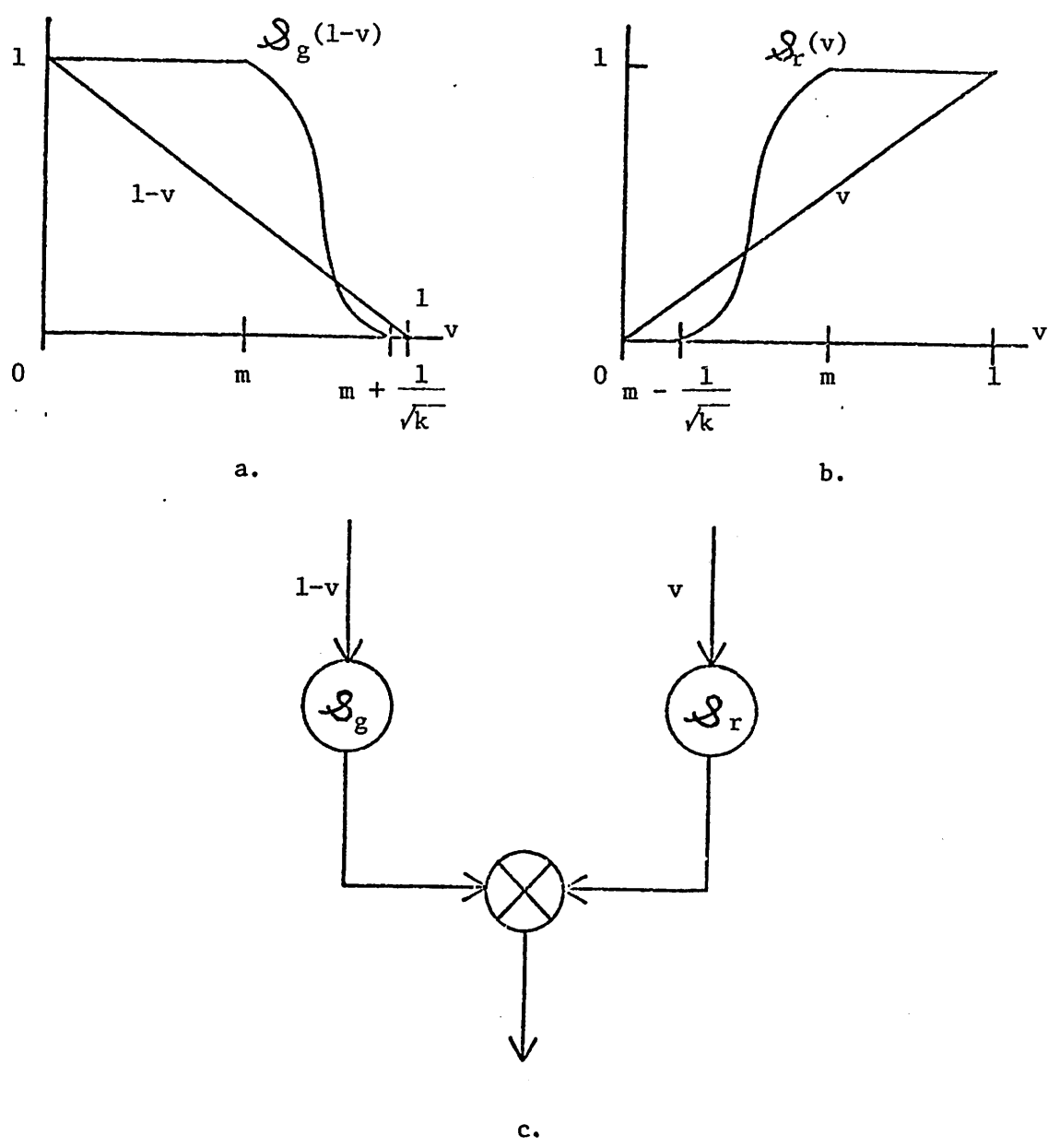


Figure 3.6 Hypothetical interneuronal circuitry to convert green saturation, $1-v$, and red saturation, v , into color coding function f_3 , by multiplying the outputs of interneurons with sigmoidal responses, \mathcal{S}_g and \mathcal{S}_r .

TABLE 3.3

The response of MMM with color coding f_3 to white test stimuli ($v = .5$) before and after alternate hue-orientation presentations.

ADAPTATION TEST		$v = 0$ $v = .5$			$v = 1$ $v = .5$			
LINE	BEFORE	AFTER	d_0	LINE	BEFORE	AFTER	d_1	
1	.507	.507	0	5	.435	.436	-.001	
2	.474	.474	0	6	.443	.427	.016	
3	.476	.484	-.008	7	.490	.487	.003	
4	.443	.444	-.001	8	.460	.450	.010	
5	.435	.442	-.007	9	.520	.466	.054	
[5	.435	.442	-.007]*	1	.507	.472	.035	
6	.443	.443	0	2	.474	.473	.001	
7	.490	.522	-.032	3	.476	.469	.007	
8	.460	.455	.005	4	.443	.448	-.008	
9	.520	.520	0	[5	.435	.436	-.001]*	
		$\bar{d}_0 = -.005$				$\bar{d}_1 = .013$		
		$\delta_0 = .011$				$\delta_1 = .020$		
	$S_\Delta = .0075$	$t = 2.368$	$df = 16$	$p < .025$		one tailed		

* duplicate results are left out of the computation.

in the f_2 version, however. The difference between the two groups is significant at the .025 level ($t = 2.368$, $df = 16$).

The f_3 version of MMM reproduces the McCollough effect without having to assume that synaptic inputs shift their spectral sensitivity with training. Of course, cortical cells still shift their sensitivity by selective training of synapses from cells with different spectral sensitivities. However, more training is required, 8 training blocks and a narrower spectral specificity of input cells, $k = 7.1$.

3.2.4. f_4 Version

A final version of the color input allowed specific tuning to a red/green ratio and seemed physiologically plausible, if not substantiated. It is a variation of equation (3.6) but normalized by the magnitude of the synaptic weights and the input:

$$f_4(v) = \frac{w_1(1-v) + w_2v}{\sqrt{w_1^2 + w_2^2} \sqrt{(1-v)^2 + v^2}} \quad (3.10)$$

This formula also has the necessary property of specific tuning to a given v_0 in $(0,1)$ as in f_2 , that is, the maximally responding cells for a fixed v_0 are those with $w_2/(w_1 + w_2) = v_0$ and the maximum response of a cell with a fixed (w_1, w_2) is at $v = w_2/(w_1 + w_2)$. The formula is symmetric in \bar{w} and v . This allows cells to be tuned to the full range of values between $v = 0$ and $v = 1$.

In this version the synaptic magnitude is held constant with normalization by a constant sum of squares instead of a constant sum. The normalization step after modification becomes:

$$s_{ik} = s'_{ik} \frac{C_s}{\left[\sum_{i=1}^{38} s'_{ik} \right]^{1/2}} \quad (3.11)$$

The thresholds in layers E and I also remain constant. (See Table 3.1 for parameter values.) To insure uniform response to color after training, the weights were chosen such that the distribution of the set of $w_2/(w_1 + w_2)$, the maximum color responses, over cortical cells was initially uniform over [0,1]. w_1 is the total synaptic strength from green R-cells and w_2 is the total synaptic strength from red R-cells. There is some evidence that the peak response of opponent-color cells is uniformly distributed over wavelength (DeValois, Abramov and Jacobs, 1966), and that cortical cells receive varying proportions of inputs from all three cone processes (Gouras, 1970a, 1970b, 1974). The 19 synaptic weights, s_{ik} , corresponding to the overall red and green input to an E-cell were then chosen randomly from a uniform distribution such that:

$$w_i = \left[\sum_{j=1+19(i-1)}^{19+19(i-1)} s_{jk} \right]^{1/2}, \quad i = 1, 2 \quad (3.12)$$

So initially the spatial specificity of E-cells was completely random and the spectral specificity was uniform, but broadly tuned.

The training procedure was the same as in the f_2 version. The network was initially exposed to a uniform distribution over orientation and saturation by presentation of two random sequences of 99 stimuli, the same set as in previous versions.

Table 3.4 shows the results of 10 ME experiments with the f_4 version. Again, the change in saturation at .5 is away from the

TABLE 3.4

The response of MMM with color coding f_4 to white test stimuli ($v = .5$) before and after alternate hue-orientation presentations.

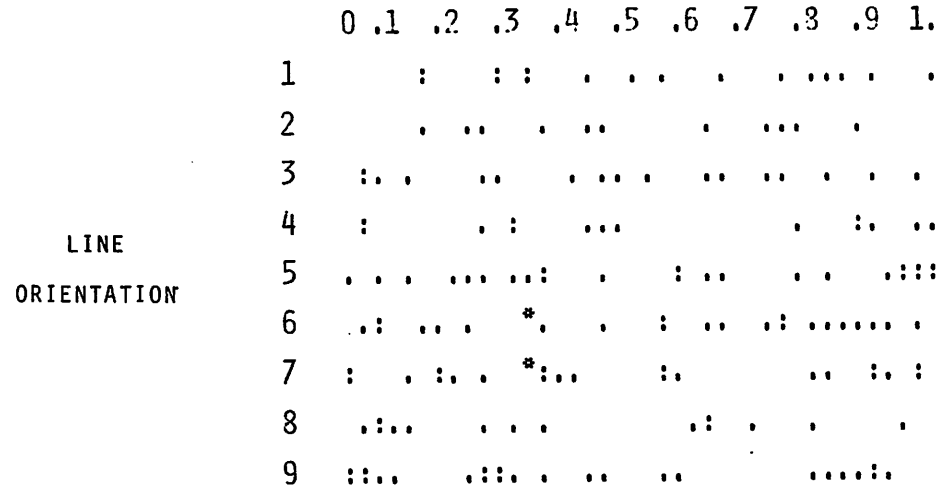
ADAPTATION TEST		$v = 0$ $v = .5$		d_0	$v = 1$ $v = .5$		d_1		
LINE	BEFORE	AFTER			LINE	BEFORE	AFTER	d_1	
1	.462	.384	.078		5	.395	.378	.017	
2	.387	.599	-.212		6	.399	.379	.020	
3	.528	.567	-.039		7	.457	.275	.182	
4	.384	.575	-.191		8	.426	.415	.011	
5	.395	.687	-.292		9	.435	.285	.150	
[5	.395	.687	-.292]	*	1	.462	.325	.137	
6	.399	.512	-.113		2	.387	.375	.012	
7	.457	.605	-.148		3	.528	.476	.052	
8	.426	.506	-.080		4	.384	.341	.043	
9	.435	.440	-.005		[5	.395	.378	.017]	*
		$\bar{d}_0 = -.111$					$d_1 = .069$		
		$\delta_0 = .114$					$\delta_1 = .068$		
	$S_{\Delta} = .0442$	$t = 4.0902$	$df = 16$	$p < .0005$			one tailed		

* duplicate results are left out of the computation.

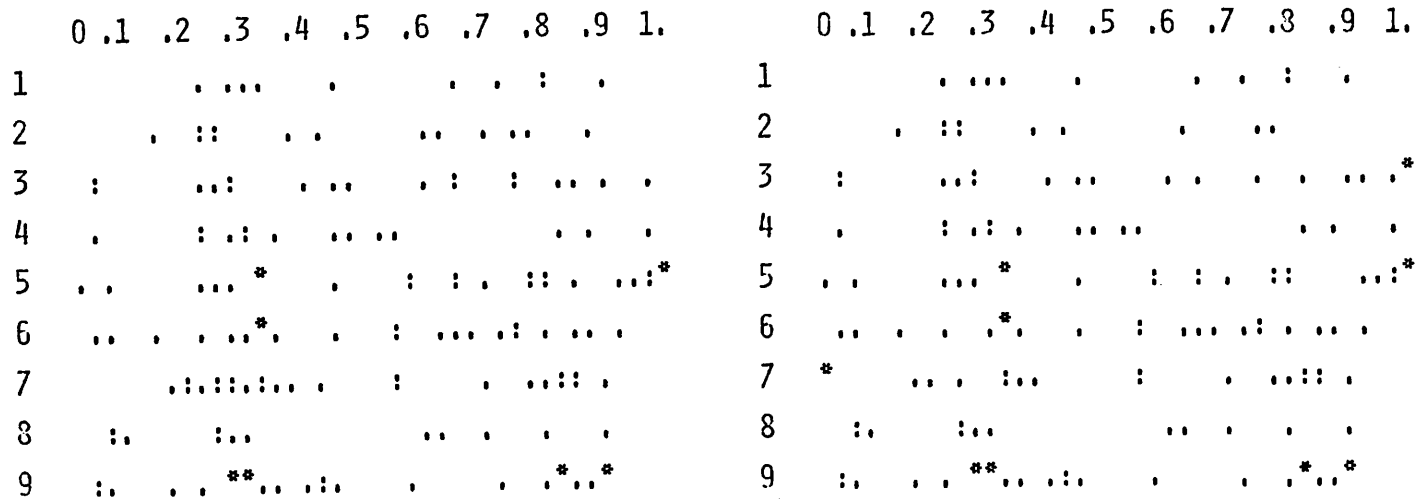
value presented during adaptation. The change in response for the two groups, one exposed to red and the other to green, is significantly different at the .0005 level ($t = 4.090$, $df = 16$). Figure 3.7 shows the distribution of cells' preferred color-orientation values before training (Figure 3.7a), after uniform training (Figure 3.7b) and after alternate presentations of line/color combinations (3.1) and (7,0.) (Figure 3.7c).

This version for color coding seems more physiologically plausible than either f_2 or f_3 . It requires no specific assignment of a color maximum for each synaptic red/green pair. It exhibits a much clearer ME than the f_3 version. The synaptic normalization scheme keeps the magnitude rather than the sum of the input and synapse vectors constant for each E-cell. This procedure more closely approximates the action of a shunting inhibition network in which the magnitude and direction of the synapse vector approaches the magnitude and direction of the input vector by synaptic modification (Grossberg, 1976).

It is interesting to note here that all attempts to reproduce the ME failed using f_4 with a uniform distribution of individual synaptic weights (UDS). With cortical cells' preferred saturation values clustered at $v = .5$, not enough cells could be drawn away from the cluster to produce a change in response at .5. The initial choice of synaptic weights had to be such that the distribution of $w_2/(w_1 + w_2)$ was uniform over cortical cells (UDC). ME presentations with this configuration produced enough of a change at $v = .5$ to exhibit the effect. The f_2 version with UDS was able to exhibit ME's because the positions of color tuning curves were much more plastic in this version. In



a.



b.

c.

Figure 3.7 Histogram of cells plotted at their preferred saturation and orientation values using color coding f_4 and synaptic weights assigned uniformly over cells. Shown are (a) the initially untrained distribution, (b) the distribution after uniform training and (c) the distribution after alternate presentations of line/color combinations (3,1.) and (7,0.).

this respect, Keith White (1976b) has found that alternate presentation of white-vertical and white-horizontal gratings before ME stimulation reduces the effect. If achromatic stimulation produces a cluster at $v = .5$ before chromatic stimulation, ME's would be reduced. The f_4 version is substantiated by these results.

3.3. Eliminating the Synaptic Conservation Rule

Grossberg (1976) argues that synaptic conservation can be generated by global properties of a network, such as shunting inhibition in pre- and post-synaptic layers, rather than by an explicit synaptic conservation rule, (3.5) or (3.11). His point is that no physiological basis for normalization exists and that it seems incompatible with classical conditioning.

In addition to these reasons for eliminating synaptic normalization, a stronger form of inhibition specific to modification was needed in order to maintain the saturation response range throughout 0 to 1. While conducting the f_4 version it was found that continued training to the uniform input set of 99 stimuli drove the response to inputs, $v = 0, 1$, toward $v = .5$ (Figure 3.8). The preferred feature histogram (Figure 3.9) after 10 training blocks, indicates that units near .5 were growing stronger than units near the extremes of the range. For example, the units that go on (represented by 0) to line 4, $v = 1$ are closer to $v = .5$ than a number of other units closer to $v = 1$. The response curves for the activated units must be higher at $v = 1$ than the units with peaks closer to $v = 1$. This means that a number of units are becoming unresponsive to all

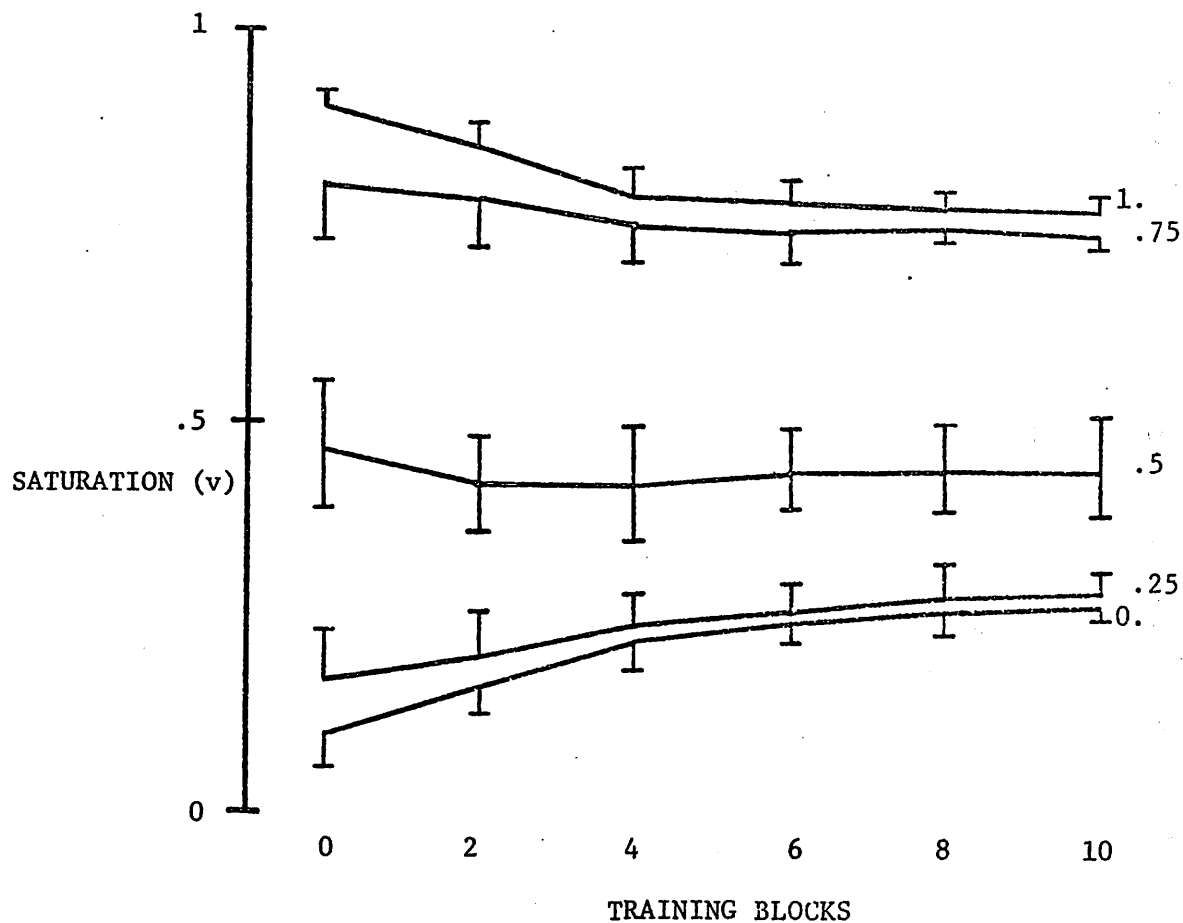


Figure 3.8 The saturation response for color coding f_4 , with 10 blocks of uniform training. The response is to input saturations indicated at the right of each curve. Each point is the average over 9 orientations, with one standard deviation indicated by the vertical bars.

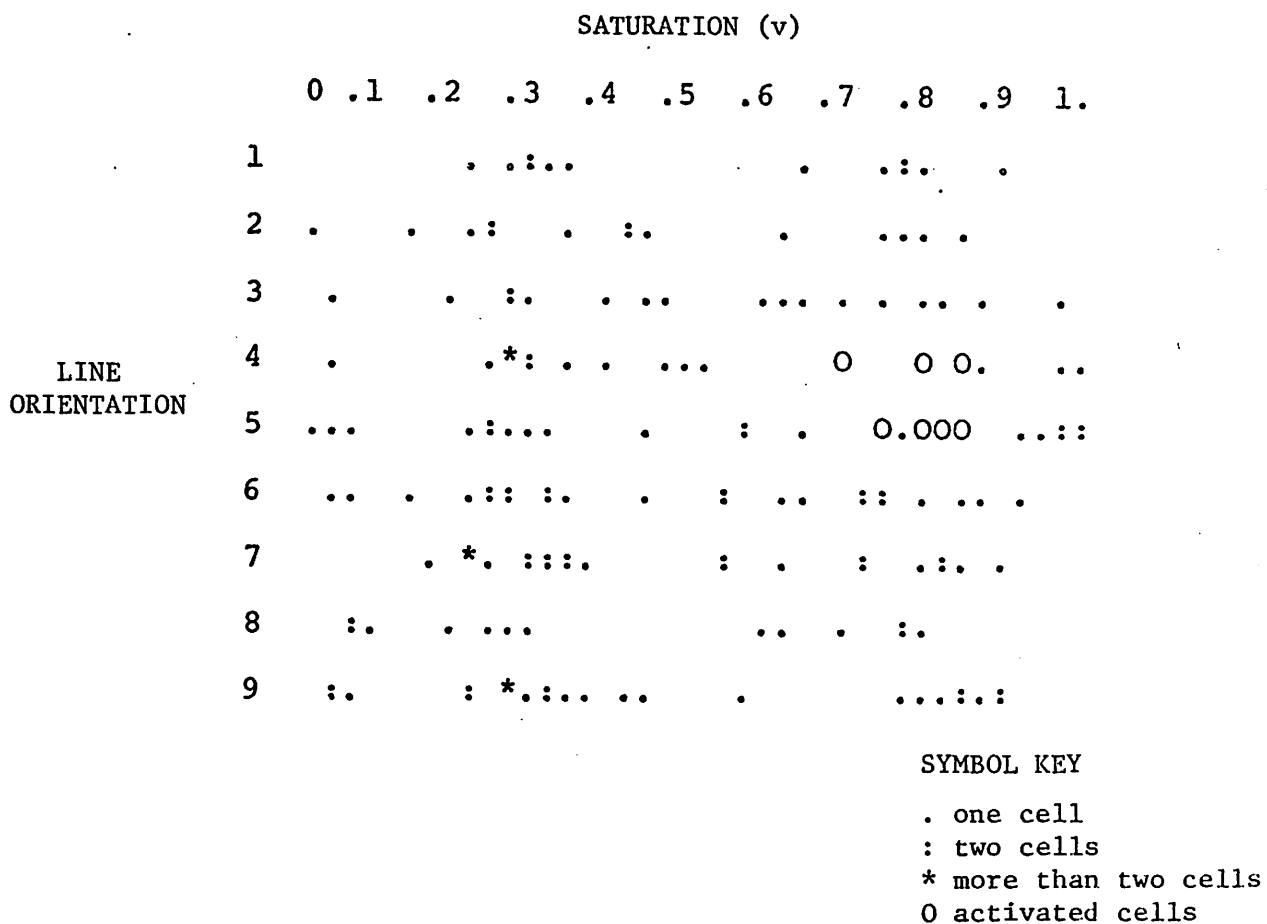


Figure 3.9 Histogram of cells' plotted at their preferred saturation and orientation values showing the response to line 4, $v = 1$. The 0's represent cells that have gone on to the input. The histogram is taken with color coding f_4 after 10 uniform training blocks.

inputs. Some form of inhibition specific to synaptic modification was needed to increase specificity without raising the peak response so high that the cell would overpower neighboring cells in feature space. It was thought that exponential decay applied to all synapses (incremented and non-incremented) when a cell became active would help the situation and allow the elimination of synaptic normalization.

3.3.1. ME's in the Untrained Network

The need for strong inhibition in MMM specific to the training of cells first became evident in a study directed at producing ME's in the untrained network. The question was whether random connectivity from layers R to E produces enough form-specificity to segregate two large enough, now-overlapping sets of cells responsive to orthogonal orientations.

The controversy of whether the ME takes place in line detectors or other, less specific form detectors (dipoles) will be discussed in Section 4.2. The following simulation was undertaken in order to show that little spatial specificity is necessary for the ME as long as there is sufficient separation between units that respond to vertical bars versus those that respond to horizontal bars. Since enough form specificity exists initially for some units to become tuned to horizontal and other units to become tuned to vertical, it was hypothesized that enough specificity exists to support a red bias in one form population and a green bias in the orthogonal population near the neutral test point.

With f_2 color coding and synaptic normalization the results of 5 ME experiments on the untrained network were equivocal, i.e., no clear effects in either direction. But the problem was not in a lack of form specificity. The problem was that the maximum response of units sensitive to the conditioning stimulus pair grew to greater than 15 times the maximum response of untrained units. So at the conditioning line orientation, units trained to $v = 0$ or $v = 1$ could also be activated by a test input at $v = .5$ and thereby swamp the activity of units near $.5$. The test response was thus strongly biased toward the conditioning saturation rather than away from it.

Some form of training rule was required that induced specificity without increasing the overall activity with respect to untrained units. A more stringent form of synaptic decay was adopted and normalization was discarded.

For this simulation all synapses decreased in proportion to E-cell activation and increased in proportion to correlation between R- and E-cell firing:

$$s'_{ik} = [s_{ik} - \alpha \Delta E_k^*]^+ + \Delta R_i^* E_k^* \quad (3.13)$$

This kept unit response curves low enough after training so that a cell tuned to $v = 0$ would not be activated by an input at $v = .5$.

The results of 10 ME experiments are summarized in Table 3.5. Specific parameters for each run are listed in Table 3.1. The results are noisier than in the uniformly trained network, but enough of an effect is present to be significant at the .05 level ($t = 1.977$, $df = 18$).

TABLE 3.5

The response of MMM with color coding function f_2 to white test stimuli ($v = .5$) before and after alternate hue-orientation presentations, starting from a spatially untrained network.

ADAPTATION TEST		$v = 0$ $v = .5$		d_0	$v = 1$ $v = .5$		d_1	
LINE	BEFORE	AFTER			LINE	BEFORE	AFTER	d_1
1	.542	.561	-.019		5	.447	.462	-.015
2	.442	.442	0		6	.437	.425	.012
3	.526	.525	.001		7	.509	.509	0
4	.451	.523	-.072		8	.500	.450	.050
5	.447	.543	-.096		9	.530	.525	.005
5	.447	.543	-.096		1	.542	.566	-.024
6	.437	.427	.010		2	.442	.438	.004
7	.509	.508	.001		3	.526	.521	.005
8	.500	.520	-.020		4	.451	.443	.008
9	.530	.533	.003		5	.447	.485	-.038
				$\bar{d}_0 = .029$				$\bar{d}_1 = .0007$
				$\delta_0 = .042$				$\delta_1 = .024$
$S_{\Delta} = .0152$				$t = 1.977$	$df = 18$	$p < .05$		one tailed

3.3.2. Attenuation of Feedback from E-Cells

Discarding the synaptic conservation rule in the f_4 version produced unstable synaptic growth. Synaptic modification was modelled by a differential equation. The discrete form:

$$s'_{ik} = \alpha s_{ik} + \Delta R_i^* E_k^* \quad (3.14)$$

was applied whenever E-cells were activated. R_i^* was always within bounds because inputs greater than 1 were never applied, however, E_k^* became unbounded due to the growth of s_{ik} . A way of limiting the positive feedback between E-cells and synapses was introduced:

$$s'_{ik} = \alpha s_{ik} + \Delta R_i^* u(E_k^*) \quad (3.15)$$

where the function, u , is of the form:

$$u(x) = \frac{u_\infty x}{x + x_0} \quad (3.16)$$

with fixed parameters: $0 < x_0 < u < 1$. u has the following properties: $u(x) \leq u_\infty$ for all $x \geq 0$ and $u(x) = x$ for $x = u_\infty - x_0$. Thus, input to s_{ik} cannot grow greater than Δu_∞ no matter how large E_k^* gets.

A number of simulation runs were tried with various choices of u_∞ , x_0 , and α (Table 3.1) but all exhibited the characteristics illustrated in Figure 3.8: decay of the response range toward $v = .5$ with increasing variance at $v = .5$. The growth of units tuned to $.5$ was still faster than that of units tuned to more extreme values. This meant that response curves at $.5$ still dominated others. It was necessary to limit overall cell response in proportion to the

number of times a cell was activated.

3.3.3. Specific Threshold Elevation

Specific threshold elevation dependent on a cell's rate of synaptic growth was tried next. The threshold, θ_k , for a cell, k , was modelled by a differential equation similar to the synaptic equation. The discrete version:

$$\theta'_k = \alpha\theta_k + g\Delta E_k^* \quad (3.17)$$

was applied to a threshold whenever the corresponding cell was activated by input.

Some preliminary simulations indicate that threshold elevation does help to maintain the response range and the separation between responses to $v = 0, .25, .5, .75, 1$ (Figure 3.10). Further investigation is needed to find a balance between the threshold time constants and synaptic time constants that produce proper separation of the response range and stability. Preliminary findings show that when the threshold gain, g , is set too high, the activity in response to $v = .5$ goes to zero with repeated training blocks, while the activity in response to $v = 0, 1$ stabilizes.

It appears that the problem of maintaining the response range and the separation between features is at least in part related to boundary effects. Cells near .5 respond to a greater range of inputs than cells at the extremes. Synaptic modification to stimuli that are very different reverses the effect of one input when the second is presented. The cell's specificity does not grow because the two

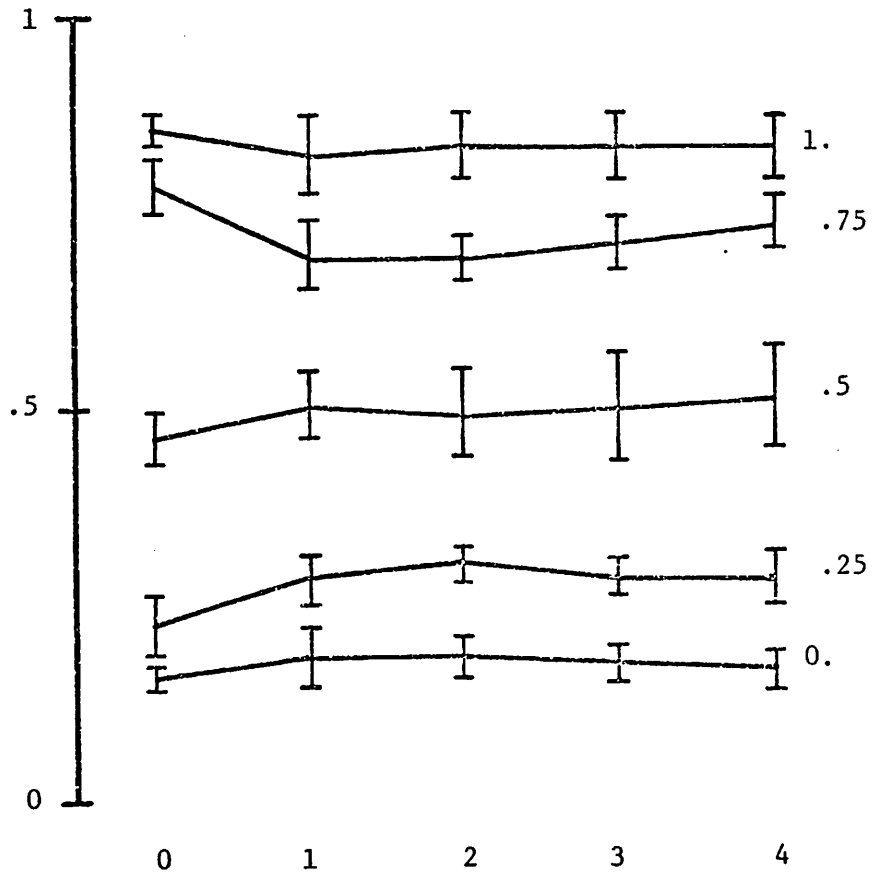


Figure 3.10 The saturation response for color coding, f_o , with threshold elevation, gain $g = 7.$, and 4 blocks of uniform training. The response is to input saturations indicated at the right of each curve. Each point is the average over 9 orientations, with one standard deviation indicated by the vertical bars.

inputs are working at cross purposes. (See Grossberg, 1975, pp. 26-30 for a discussion of this problem.) Even though the range is kept small by threshold elevation, the maximum response cannot grow. Cells near the boundary with a smaller range of inputs receive synaptic increments in the same direction, and thus become strong to a smaller set of inputs.

A way of getting around the discontinuous boundary problem is to make the color dimension a continuous ring similar to line orientation. Then the input range over all values of v is the same size. Implications of a wrap-around color dimension are discussed in Section 4.3.

3.4. Model Modelling

At a certain point in a large computer simulation sub-problems come up that are more easily solved by sub-simulations. A large complex simulation helps to point out new directions for research and to demonstrate unexpected effects. But when too many new effects swamp the perception of desired effects it is time to build a more tractable model of a subpart of the larger problem.

MMM was instrumental in exploring feature extraction in two dimensions. It demonstrated that with a uniform input set the response curves to specific orientations and saturations became more narrowly tuned. An unanticipated result, derived from the organization of the input layer and the random connectivity to E, was that color and form specificity are inversely related. That is because the probability that receptive field (R) cells line up in a given line orientation

and all have the same spectral specificity is extremely low. Either one specificity or the other dominates. Another unanticipated finding was that inhibition must be increased specifically for trained cells so that newly modified cells do not dominate the unspecified cells. Fatigue immediately after conditioning may have a computational purpose. But beyond a certain point the network effects became excess baggage to the investigation of feature space transformations. A smaller version that would embody just the salient aspects of response curve tuning and modification was required without the added problems of the statistics and dynamics of 376 interconnected cells and 6422 modifiable synapses.

The simulation outlined in section 2.1.4. (program TUNE) simulates the three response curve modifications present in MMM resulting from synaptic changes: shifting toward the input, narrowing of the tuning curve, and heightening of the peak response. The fourth type of change included one that was never properly implemented in MMM but was more easily incorporated into TUNE: threshold elevation. These four types of modification capture the feature space tuning aspects of MMM. In the smaller program, positive and negative aftereffects were isolated with respect to two output measures: total activity (2.2) and featural response (2.7). It was seen that these two outputs of the network are very different. They are related but they can go in opposite directions depending on the relative amounts of the four types of modification, i.e., negative featural aftereffects do not necessarily imply reduced activity (Figure 3.11). Many investigators seeking models of featural aftereffects have assumed that the two are one and the same. Total activity may be a useless indi-

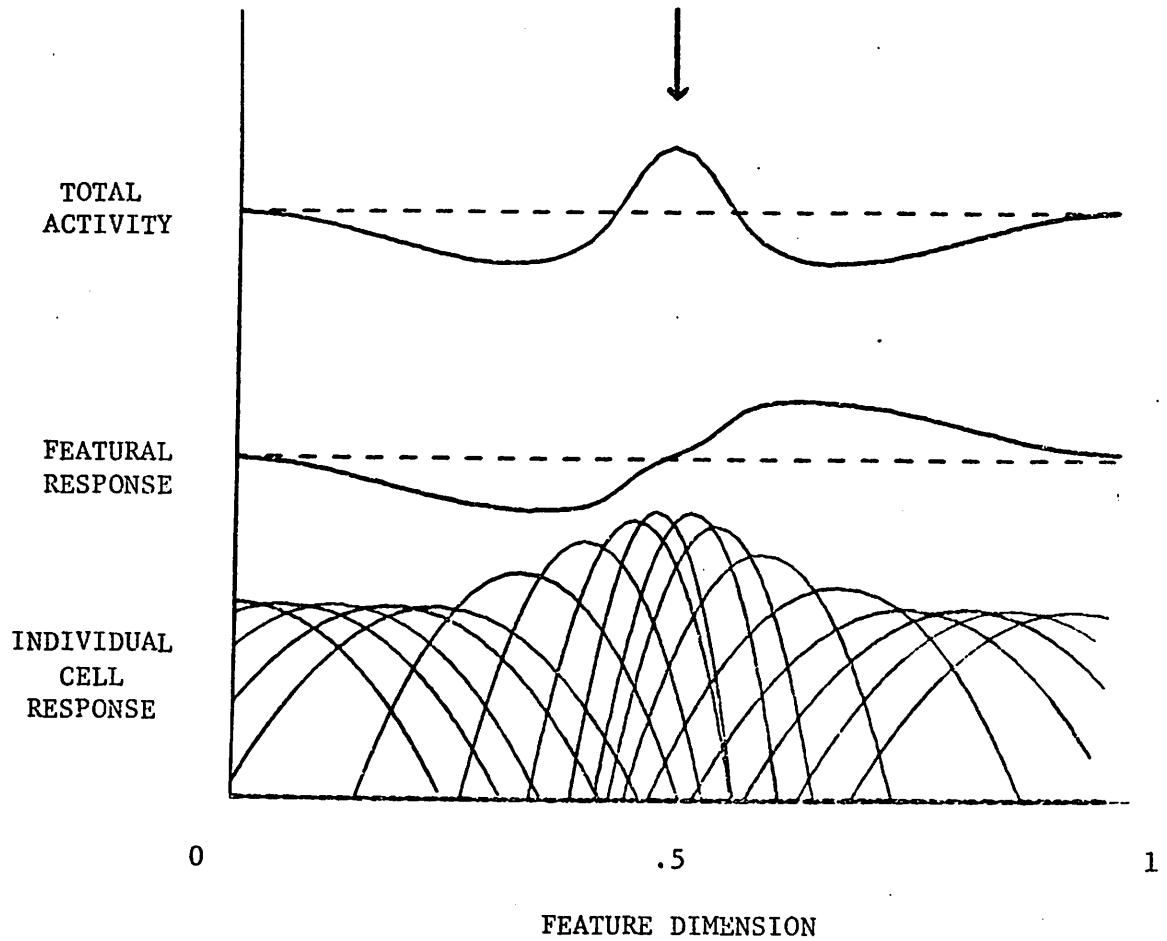


Figure 3.11 The changes in the total activity and featural response produced by shifting, narrowing, and heightening of individual response curves near the modifying stimulus. Note the increase in total activity at v_m with negative aftereffects near v_m . $\omega = .5$, $v_m = .5$, $\Delta_x = .5$, $\Delta_\omega = .15$, $\Delta_h = .5$, $\Delta_\theta = 0$.

cator of long-term featural aftereffects, especially in a network having inhibitory interactions designed to keep total activity constant. TUNE clearly illustrates the different effects that changing tuning curve parameters can have on activity and featural response. Besides being more tractable, TUNE is faster, less noisy and more efficient. For investigating feature space tuning along one dimension it is better than MMM, but it loses unit interconnection properties, dynamic properties, and statistical properties of the larger simulation.

The two questions that must be answered before undertaking a large simulation are 1) at what level of representation does one wish to address the problem, and 2) what is the minimal model that embodies just the characteristics of the problem under investigation?

C H A P T E R I V
CONTINGENT-AFTEREFFECT MODELS

4.1. Are Color and Form Coded Separately or Together?

An excellent review of current models of the ME can be found in Skowbo, et. al., (1975). The review classifies existing models into several non-mutually-exclusive categories. Two categories which are mutually exclusive are the single-unit models versus the multiple-unit models. Single unit models assume that the effect occurs in form-specific cells either broadly tuned (achromatic) or narrowly tuned (chromatic) to wavelength.

The achromatic form-detector model assumes a decrease in sensitivity to the color to which units have been exposed, that is, part of the color range of form-specific cells is depressed. This model is really a two-stage or multiple-unit model in disguise. Form-specific detectors are achromatic by virtue of receiving input from several cone processes: red, green, and blue (Gouras, 1972). Loss of sensitivity to a specific wavelength contingent on specific form cannot occur without linking form-specificity and color-specificity through feedback or through coding of both features in the same cell. The former explanation puts this model into the multiple-unit category, and the latter explanation puts it into the double-duty, single-unit category. Achromatic, form-specific, single-unit models cannot support contingent aftereffects.

Loss of sensitivity of double-duty units, on the other hand, has not been substantiated by experiments using controls for after-images. Adaptation to complementary chromatic gratings produces

form-specific but not color- and form-specific threshold elevation (Timney, et. al., 1974). It was once thought that only very few cells in cortex were specific for both color and form (Hubel and Wiesel, 1968) but Peter Gouras (1972, 1974) has found that color- and form-specificity vary inversely in single cortical cells with about 28% in the middle category, having some degree of specificity for both features. These units which could correspond to E-cells in the present model could support CAE's, but whether loss of sensitivity is the primary mechanism underlying these effects is another question.

Most proponents of a two-stage model of the ME do not mention feedback between units. Without feedback depression of color-specific cells or pathways before form-specific cells affects all form cells uniformly. Similarly, for a two-stage model where form is coded before color, depression of a specific color response affects the form response uniformly. Two-stage models cannot work without synaptic modification of feedback connections between the two populations. Creutzfeldt (1973) has proposed a two-process model with feedback through inhibitory connections that increase with activation. This is probably as good a model as MMM except that loss of sensitivity to colored gratings does not always accompany ME's (Timney, et. al., 1974).

4.2. Form-Specificity

Two kinds of questions arise in regard to the type of form-specificity necessary for orientation-contingent ME's: 1) is form-specificity dependent on spatial frequency detectors or size detectors;

and 2) is it dependent on line detectors or a more amorphous type of luminance change detector?

First, it is very difficult to distinguish spatial frequency detectors from bar detectors behaviorally. Bar detectors, i.e., with excitatory central regions and inhibitory flanks, are broadly tuned to spatial frequency. They exhibit all of the characteristics attributed to spatial frequency detectors (Macleod and Rosenfeld, 1974; Legény, 1975). Narrowly tuned spatial frequency detectors of the type necessary for a Fourier transform model of visual perception have not been found. However, Harris (1971) has shown that ME's depend on periodicity, not on the sizes of black or white bars in $1/3$ and $2/3$ duty cycle (ratio of white bar width to period) square wave gratings. If bar detectors are most responsive to bar width one would expect ME's to depend on the width of black or white bars not on the period. This argument is not necessarily correct given a population of bar detectors without sharp transitions between on and off areas and with enhancing connectivity among units of equal-size bar widths. Suppose that equal-size black bar detectors (off-center and on-flanks) and white bar detectors (on-center and off-flanks) are positively coupled to fire as a population such that the activity of the population is averaged over the activity of black and white bar detectors (irrespective of the phase relations between them). Then the size population maximally sensitive to a $2/3$ duty cycle square-wave grating is the population whose receptive fields fit the period of the grating rather than the width of either white or black bars (see Appendix B).

In another set of experiments (May and Matteson, 1976; Green, Corwin and Zemon, 1976) the authors conclude that spatial frequency-

specificity rather than edge-specificity underlies ME's. In these experiments subjects were presented alternating red and green checkerboards respectively aligned to vertical and to 45° off vertical. The ME was tested with square-wave gratings of various spatial frequencies and orientations. Maximal ME's were produced with gratings tilted 45° with respect to the inducing pattern and having a period $\sqrt{2}$ times the size of the squares in the pattern. This apparently favors a Fourier transform hypothesis because the strongest Fourier component of a checkerboard is precisely one with a period $\sqrt{2}$ the square size aligned diagonally to the pattern. However, bar detectors again can explain these results.

Assume the existence of bar detectors with equal sized on- and off-regions with weights +1 for the excitatory region and -.5 for each of the inhibitory regions. Also assume a linear response for partial stimulation within these regions. In order for contingent aftereffects to occur with test gratings 45° of angle apart there must be a difference in the amount that a bar detector is adapted by a checkerboard orthogonally aligned to its receptive field versus a checkerboard diagonally aligned. The population of bar detectors with the greatest absolute difference in response to a checkerboard oriented orthogonally and diagonally will produce the greatest contingent aftereffect. The sign of this difference will determine the direction of the color aftereffect.

Let us consider the strength of the effect produced by a bar detector having the same width as the squares in the checkerboard, aligned orthogonally versus that of a bar detector $1/\sqrt{2}$ the square size, aligned diagonally. We can plot the effect of these two populations as a func-

tion of the ratio of bar length to width, r , and observe which of the effects is greater for which values of r .

The response of a bar detector having an excitatory region the same width as the square size, aligned orthogonally to the pattern, O_1 , minus the response of one aligned diagonally, D_1 , is plotted in Figure 4.1 (dashed line) as a function of r . As r increases the difference goes negative, i.e., the diagonally aligned detector produces a greater response than the orthogonally aligned detector beyond $r = 5$. However, the response of a bar detector of width $1/\sqrt{2}$ the square size, aligned diagonally, D_2 , minus that of one aligned orthogonally, O_2 , (solid line) is above $O_1 - D_1$ for $r > 1.8$. Since most bar detectors have a length to width ratio at least greater than 1.8 (see footnote 1), the greatest contingent aftereffect is supported by diagonally aligned bar detectors having widths $1/\sqrt{2}$ the size of the check pattern. In fact, for $2 \leq r \leq 4$, the range in which most bar detectors lie, $O_1 - D_1$ is positive in less than half the range. Furthermore, at $r > 6$ diagonally aligned receptive fields for both bar widths produce the greater response. (See Appendix C for calculations.)

The experimental findings do eliminate the possibility that edge detectors, units having one excitatory and only one inhibitory region, play a significant role in this aftereffect, however bar detectors with two inhibitory flanks on either side can explain this spatial frequency related effect, quite adequately.

The second question concerning form-specificity deals with the degree of form-specificity necessary for ME's. Harris and Gibson

¹ Bar detectors with $r < 1.8$ approximate square-shaped or concentric receptive fields which could not very well support orientation-specific adaptation.

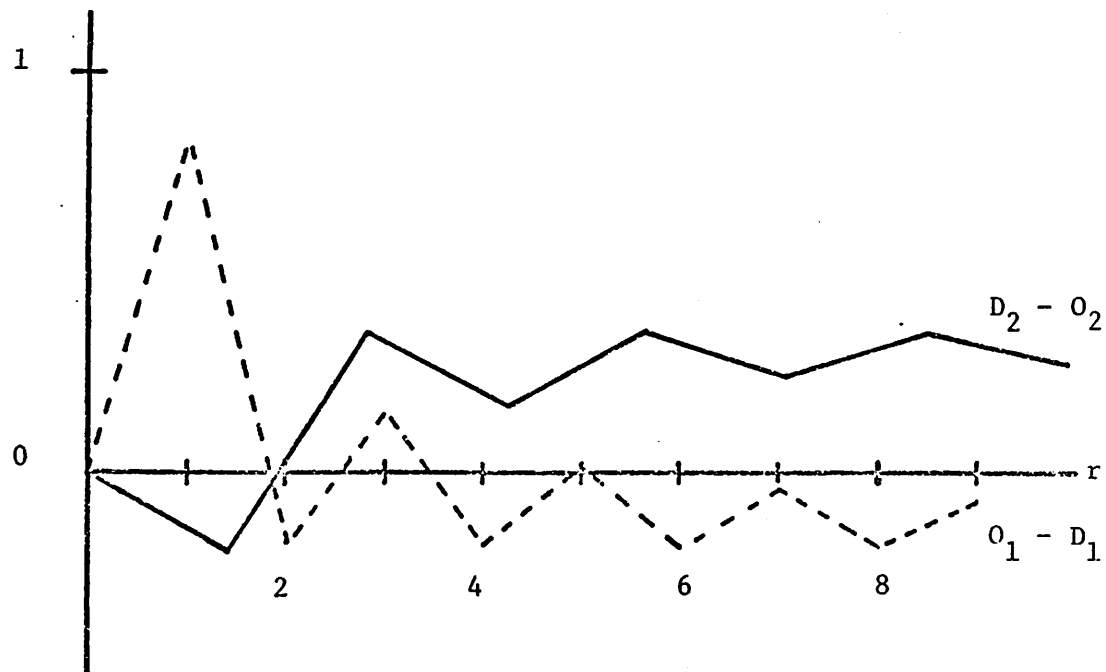


Figure 4.1 The response of bar detectors the same width as the squares in a checkerboard pattern when aligned orthogonally minus their response when aligned diagonally to the pattern (dashed line). The response of bar detectors $1/\sqrt{2}$ the width of the squares when aligned diagonally minus their response when aligned orthogonally to the pattern (solid line). These are plotted as a function of r , the bar length to width ratio.

(1968a, 1968b) proposed a minimal form detector for ME's called the "dipole." The dipole is a unit having only two retinal points in its receptive field: one on-unit and one off-unit separated by a vector. The direction and size of the vector specify the unit's orientation and size specificity, but one much more broadly tuned than for bar or edge detectors with sharp, straight line boundaries between on- and off-regions. The f_4 version of the MMM simulation of ME's in the untrained network indicates that, at least theoretically, broadly tuned form specificity will suffice. But, experimentally, color-contingent tilt-aftereffects (Held and Shattuck, 1971) show that maximal effects occur when adaptation stimuli are tilted 15° in either direction from vertical. This indicates a relatively narrowly tuned orientation detector with a tuning width on the order of 30° . Dipoles, on the other hand, have orientation tuning widths of 180° .

The logical construct of the dipole serves as a minimal edge detector (one transition from light to dark) but experiments showing the supremacy of periodicity over size (Harris, 1971) and bars (two transitions) over edges (May and Matteson, 1976; Green, Corwin and Zemon, 1976) require a minimal bar detector. Bar detectors with sloping transitions between on- and off-regions and with equal area on- and off-regions are specific enough to orientation and spatial frequency to explain all spatial frequency effects associated with ME's.

4.3. Is Color a Dimension?

Line (bar and edge) detectors are uniformly distributed over all orientations (Hubel and Wiesel, 1962). The response to a particular orientation is in terms of which set of units is firing the most. Orientation is represented by the activated units weighted by firing rate (Section 2.1.4.). But does color work this way or is it more like luminance? The measure of luminance is simply the level of firing of a luminance-sensitive unit. Analogously, is color merely the amount that a red or green cell fires rather than the weighted average of units with tuning curves distributed continuously throughout wavelength?

DeValois, Abramov, and Jacobs (1966) categorize narrowly tuned, color sensitive cells in LGN into four categories: +R-G, +G-R, +Y-B, +B-Y, where + represents excitatory, - inhibitory, R red, G green, Y yellow, and B blue. Their basis for classification is the distribution of zero crossings (point of transition from excitation to inhibition) of spectral tuning curves. The histogram of crossover points plotted against wavelength is roughly bimodal with a minimum at 560 nm. +R-G and +G-R crossover above 560 nm, and +Y-B and +B-Y crossover below 560 nm. In their analysis they are able to reject the hypothesis, with probability .05, that units excited by long wavelengths (+R-G, +Y-B) come from a uniform distribution, but they were unable to reject it for units excited by short wavelengths (+G-R, +B-Y). The short wavelength distribution appears roughly uniform (DeValois, Abramov and Jacobs, 1966, Figure 4). The authors state that peak sensitivities are even more variable than crossovers and appear to

be continuously distributed over wavelength. In spite of their warnings about the possibly arbitrary nature of the categorization, later researchers take it for granted that color-opponent cells are neatly divided into four categories. No one after DeValois, Abramov and Jacobs addresses the question directly. A later study by Gouras (1974, Figure 11), however, shows a wide variation in peak spectral sensitivities in monkey striate cortex. So at least for pure color, wavelength may be thought of as a dimension to the visual system analogous to line orientation (Figure 4.2).

If color units are distributed continuously along a color dimension it should be possible to test for the tuning width of these units in color feature space just as Held and Shattuck (1971) isolated the tuning width of units along orientation. They showed that maximal color-contingent tilt-aftereffects occur with red and green gratings tilted respectively 15° left and right of vertical. The equivalent experiment in the color domain would be to vary the saturation purity of adaptation (A) stimuli while testing (T) at white (Figure 4.3a). A monotonic increase in the effect with saturation purity would indicate either very broadly tuned color units or a scalar representation for color. Some pilot studies by White (1976c) show a monotonic increase with saturation purity in experiment 1 (Figure 4.3a). But preliminary findings of a second experiment (Figure 4.3b) in which the adaptation stimuli are white and test stimuli are desaturated colors seem to indicate that the strength of the aftereffect is not strictly a monotonic function of the distance between A and T, but may depend on the absolute values of A and T also (White, 1976d). If the function for ME versus saturation difference between A and T rises and

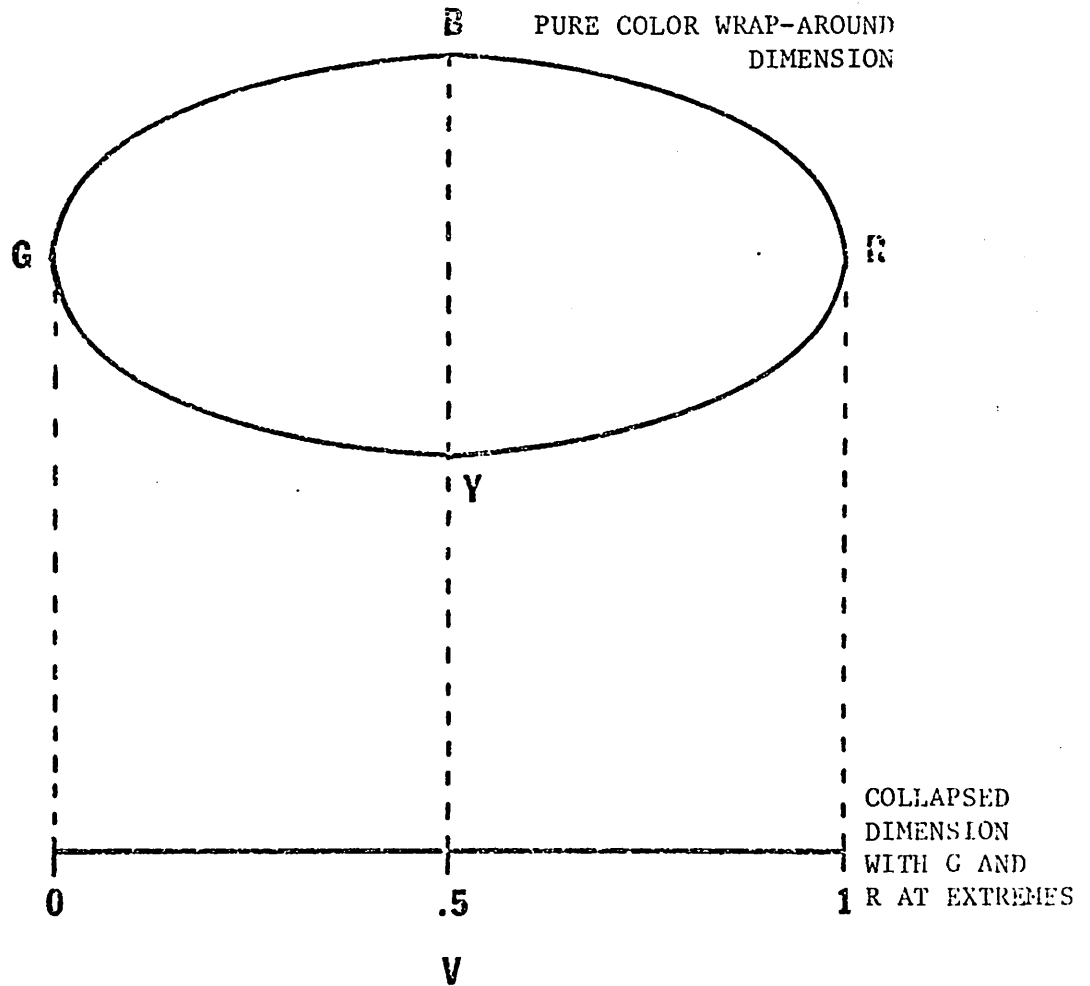
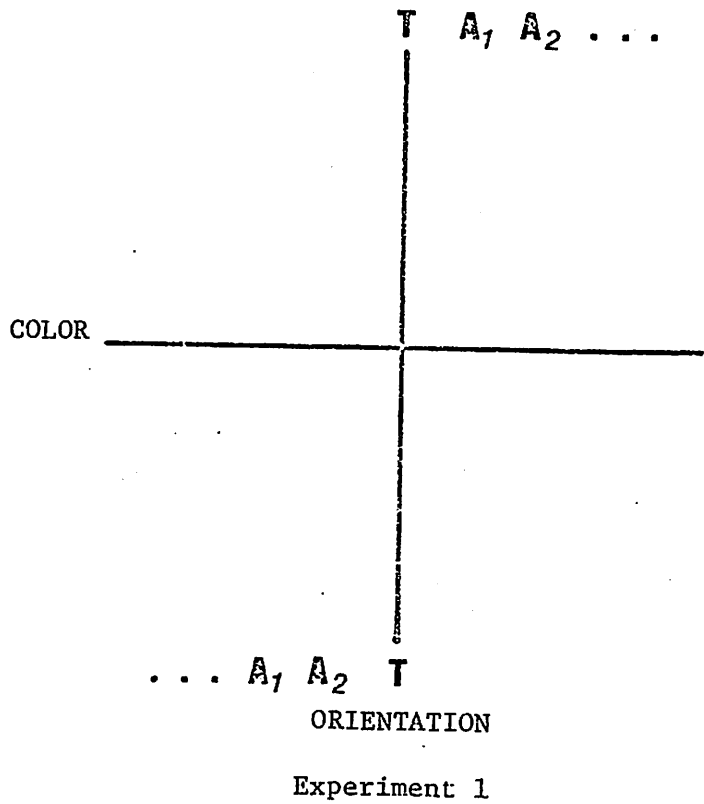
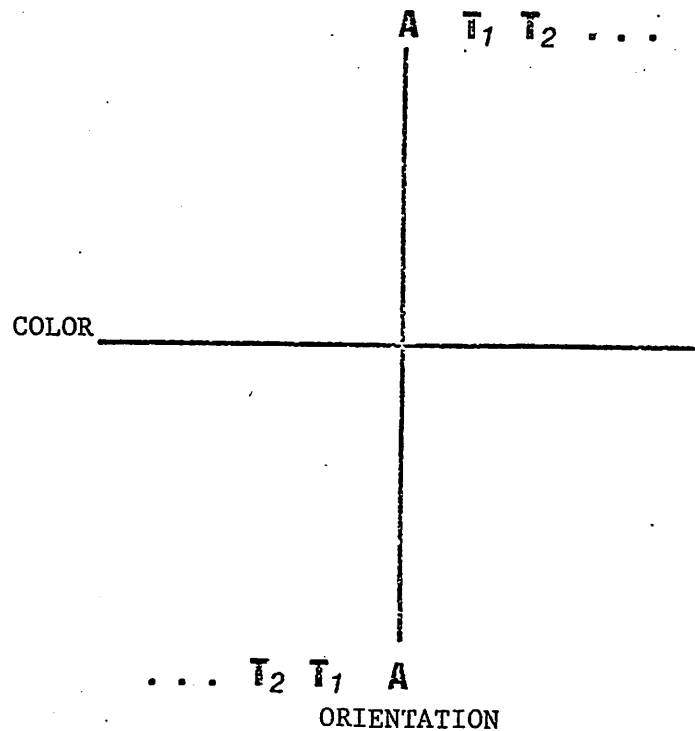


Figure 4.2 The saturation dimension can be thought of as a collapsed, pure color, wrap-around dimension in which blue and yellow coincide to produce white ($v = .5$), and green ($v = 0$) and red ($v = 1$) are located at the extremes.



Experiment 1

a.



Experiment 2

b.

Figure 4.3 Two parametric experiments to test for tuning width along the color dimension. A corresponds to the adaptation stimulus and T to the test in color/orientation space.

then falls (negative aftereffect), or falls and then rises (positive aftereffect) the distance at which an effect is no longer present would determine the width of saturation-sensitive units.

One difficulty with this set of experiments is that the purity scale may be too short with respect to unit tuning widths to reveal a U-shaped aftereffect function. An equivalent set of experiments should be tried on the wrap-around, pure color dimension discussed above. In this case, the distance in color space between A and T can be varied up to half the dimension, as opposed to only 1/4 the dimension in the collapsed version using white A's or T's (Figure 4.2). A's and T's would always be pure colors with no variation in saturation purity. A few experimenters have varied the wavelength of A's to other values beside strict complementary combinations but T's have always been white (Stromeyer, 1969; Murch and Paulson, 1976). Mixing saturation purity of A's and T's may confound experiments designed to find the tuning widths of color units, since tuning widths along wavelength increase with decreasing purity (DeValois and Marrocco, 1973).

In this regard, U-shaped unit response curves for pure color appear to be well established physiologically (DeValois, Abramov and Jacobs, 1966) but no evidence for U-shaped unit responses along saturation purity exists.

A P P E N D I X A

DISCRIMINABILITY IN A DISTRIBUTION OF FEATURE SENSITIVE UNITS
WITH QUADRATIC TUNING CURVESUniform Activity.

Given a uniform distribution of n detectors, equally spaced over $v \in [0,1]$, with equal tuning widths, ω , heights, h , and tuning curves:

$$a_i(v) = h \left[1 - \left(\frac{v - f_i}{\omega} \right)^2 \right], \quad f_i = \frac{i}{n},$$

The total activity is given by:

$$A(v) = \sum_i a_i(v) =$$

$$h \left[1 + \sum_{k=1}^m 2 \left(1 - \left[\frac{v - (v + k/n)}{\omega} \right]^2 \right) \right], \quad \text{for } v = \frac{1}{n}, \frac{2}{n}, \dots, 1$$

where $m = \text{int}[\omega n]$ (the function "int" returns the greatest integer less than or equal to the argument). $A(v)$ reduces to:

$$A(v) = h \left[1 + 2m - \frac{1}{(\omega n)^2} \left(\frac{m(m+1)(2m+1)}{3} \right) \right].$$

Discriminability.

Given a non-uniform input distribution, $g(v)$, and a non-uniform set of tuning curves with parameters given by:

$$h_i = 1,$$

$$\omega_i = \frac{\omega_0}{g(x_i)},$$

and

$$x_i - x_{i-1} = \frac{f_i - f_{i-1}}{g(x_i)}$$

where $\bar{g}(v)$ is a smoothed version of $g(v)$ [equation (2.8)], then

$$\text{int}\left[\frac{\omega_0}{f_i - f_{i-1}}\right] = \text{int}\left[\frac{\omega_i}{x_i - x_{i-1}}\right] = m.$$

For $m = 1$, $A(v) = 1$, and the discriminability is given by:

$$\frac{dR(v)}{dv} \cong \frac{R(x_i) - R(x_{i-1})}{x_i - x_{i-1}} = \frac{f_i - f_{i-1}}{x_i - x_{i-1}} = \bar{g}(x_i).$$

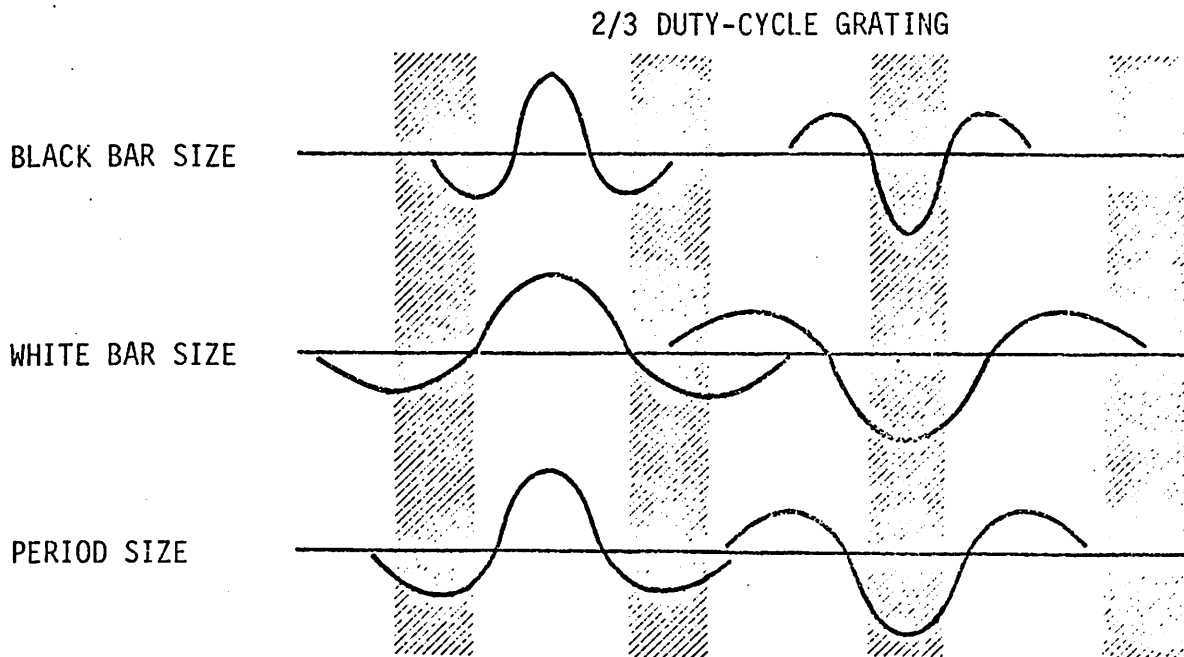
For $m = 2$, $A(v) = \frac{5}{2}$, and

$$\begin{aligned} \frac{dR(v)}{dv} &\cong \frac{R(x_i) - R(x_{i-1})}{x_i - x_{i-1}} \\ &= \frac{2}{5(x_i - x_{i-1})} \left[f_{i-1} \left(1 - \left[\frac{x_i - x_{i-1}}{\omega_{i-1}}\right]^2\right) + f_i + f_{i+1} \left(1 - \left[\frac{x_i - x_{i+1}}{\omega_{i+1}}\right]^2\right) \right. \\ &\quad \left. - f_{i-2} \left(1 - \left[\frac{x_{i-1} - x_{i-2}}{\omega_{i-2}}\right]^2\right) - f_{i-1} - f_i \left(1 - \left[\frac{x_{i-1} - x_i}{\omega_i}\right]^2\right) \right] \\ &\cong \frac{2}{5(x_i - x_{i-1})} \left[f_{i-1} \left(1 - \frac{1}{m^2}\right) + f_i + f_{i+1} \left(1 - \frac{1}{m^2}\right) \right. \\ &\quad \left. - f_{i-2} \left(1 - \frac{1}{m^2}\right) - f_{i-1} - f_i \left(1 - \frac{1}{m^2}\right) \right] \\ &= \frac{2}{5(x_i - x_{i-1})} \left[\frac{3}{4}(f_{i-1} - f_{i-2}) + (f_i - f_{i-1}) + \frac{3}{4}(f_{i+1} - f_i) \right] \\ &\cong \frac{2}{5} \left[\frac{3}{4} \bar{g}(x_{i-1}) + \bar{g}(x_i) + \frac{3}{4} \bar{g}(x_{i+1}) \right] \\ &\cong \frac{2}{5} \left(\frac{5}{2} \bar{g}(x_i) \right) = \bar{g}(x_i). \end{aligned}$$

So for small m and small $\bar{g}(x_i) - \bar{g}(x_{i-1})$ the discriminability is approximately equal to $\bar{g}(v)$.

A P P E N D I X B

SPATIAL-FREQUENCY-LIKE BAR DETECTORS



PERCENT STIMULATION

DETECTOR SIZE	POS.	NEG.	AVG.
BLACK BARS	41	100	71
WHITE BARS	59	59	59
PERIOD	83	88	85

Suppose that bar detectors have cross sections as illustrated in the figure, and suppose that we simulate them with the second derivative of a Gaussian function for ease of calculation. Let the positive region equal +1 and the negative regions together equal -1, when totally stimulated by white. Also, let the width of the excitatory region

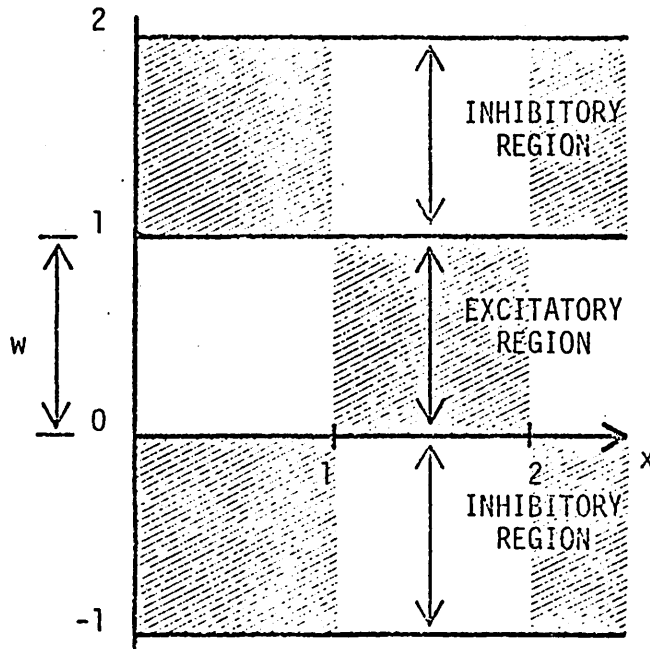
equal the width of each of the inhibitory flanks, i.e., the Gaussian is truncated at $\pm 3 \sigma$.

Suppose that positive (white bar) and negative (black bar) detectors are coupled¹ such that the average activation of positive and negative units determines the efficacy of a stimulus, then the population fitted to the period is activated more than either the population fitted to black bar size or white bar size (see figure and table above). A similar argument applies also for a 1/3 duty-cycle grating.

¹ The detectors may be coupled through positive feedback loops such that they fire as a population. Note that this arrangement does not require any particular phase relation between individual receptive fields.

APPENDIX C

ACTIVATION OF BAR-SHAPED RECEPTIVE FIELDS BY CHECKERBOARDS



$$O_1, w = 1.$$

Given a checkerboard pattern with a square size of 1, an orthogonally aligned, bar-shaped, receptive field with excitatory width, $w = 1$, weighted by 1, and inhibitory flanks of equal widths,

each weighted by -0.5 , the area integrated by such a receptive field is equal to x in the interval $[0,1]$ and $2 - x$ in the interval $[1,2]$.

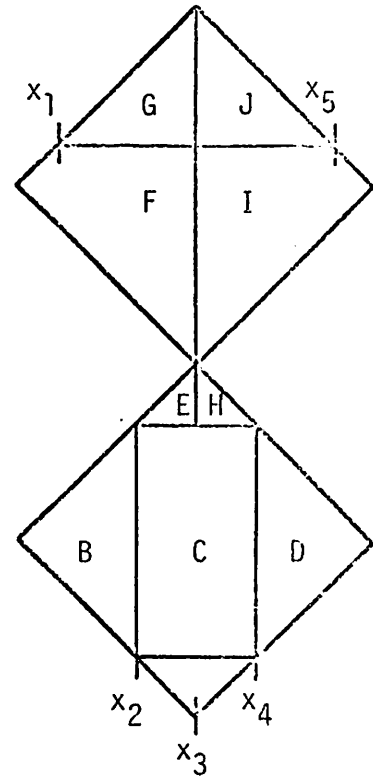
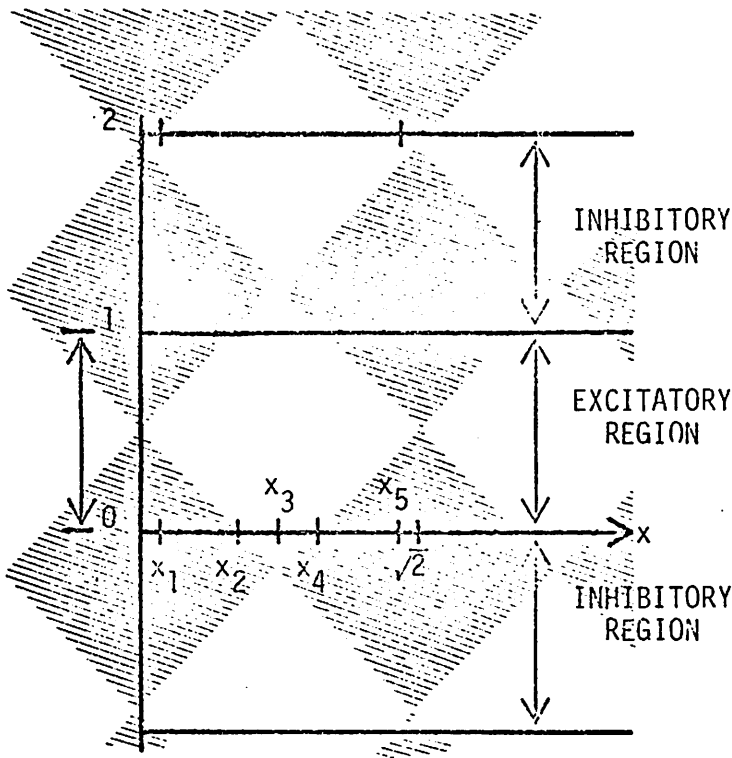
In general the weighted area is equal to:

$$A = \begin{cases} x - n & \text{for } n \text{ even} \\ n + 1 - x & \text{for } n \text{ odd} \end{cases}$$

where $n = \text{int}(x)$. If we normalize the integrated area by excitatory receptive field area, rw , and substitute the bar length to width ratio, $r = x$, for x we obtain the response:

$$O_1 = \begin{cases} \frac{r - n}{r} & \text{for } n \text{ even} \\ \frac{n + 1 - r}{r} & \text{for } n \text{ odd} \end{cases}$$

as a function of r for a bar aligned orthogonally to a checkerboard pattern.

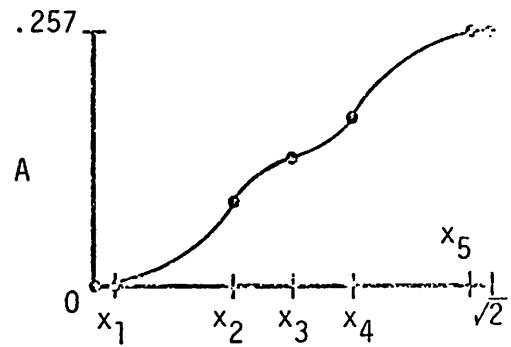


$D_1, w = 1.$

For a diagonally aligned receptive field, $w = 1$, the area calculation may be simplified by substituting the top inhibitory region weighted by -1 in place of two regions each weighted by $-.5$, since the two areas are symmetrical. The area integrated within one cycle of the check pattern, $x \in [0, \sqrt{2}]$, is given by:

$$A = B + C + D - E - H - (F - G) - (I - J)$$

$$= G - 3E + J - 3H.$$



$A(x)$ is a monotonic increasing, piecewise quadratic function of x , as illustrated in the above graph. $A(x)$ can be approximated by a linear

function with slope $3(\sqrt{2} - 1)^2/(2\sqrt{2})$, which is the area integrated by the receptive field within one cycle of the pattern. If we normalize A by the excitatory area, rw , and substitute $r = x$ we obtain the response:

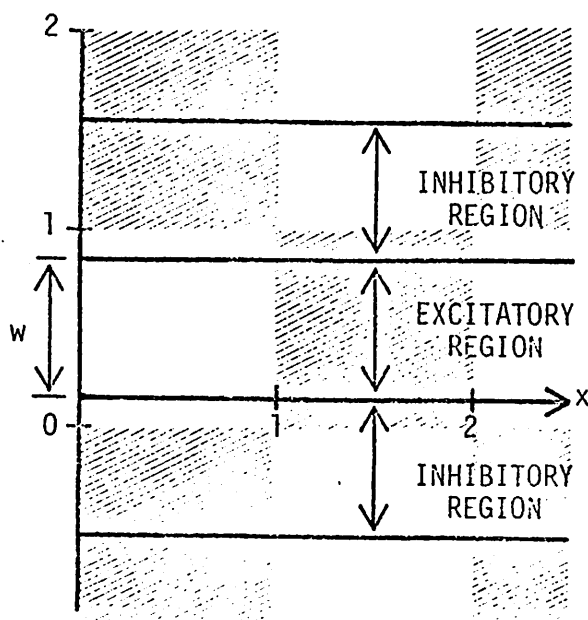
$$D_1 \cong \frac{9 - 6\sqrt{2}}{2\sqrt{2}}$$

of a bar detector aligned diagonally to the pattern.

$$O_2, w = 1/\sqrt{2}.$$

The area integrated by a receptive field, $w = 1/\sqrt{2}$, aligned orthogonally to the check pattern is given by ax in the interval $[0,1]$ and by $a(2 - x)$ in the interval $[1,2]$, where

$$a = \frac{3 - \sqrt{2}}{2\sqrt{2}}.$$



In general:

$$A = \begin{cases} a(x - n) & \text{for } n \text{ even} \\ a(n + 1 - x) & \text{for } n \text{ odd} \end{cases}$$

where $n = \text{int}(x)$. Substituting $x = r/\sqrt{2}$ and normalizing by rw we obtain:

$$O_2 = \begin{cases} \frac{a}{r}(r - n\sqrt{2}) & \text{for } n \text{ even} \\ \frac{a}{r}(n\sqrt{2} + \sqrt{2} - r) & \text{for } n \text{ odd} \end{cases}$$

for the response of an orthogonally aligned receptive field.

$$D_2, w = 1/\sqrt{2}.$$

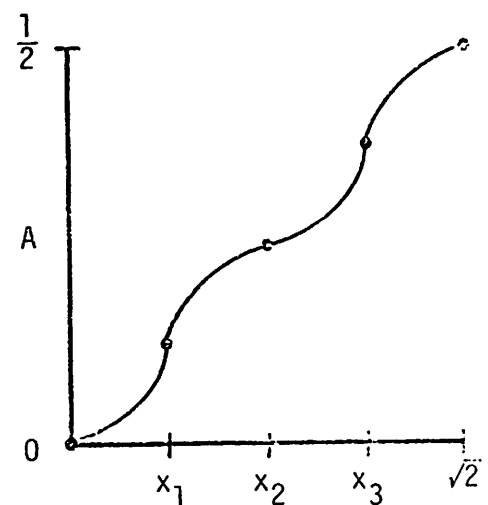
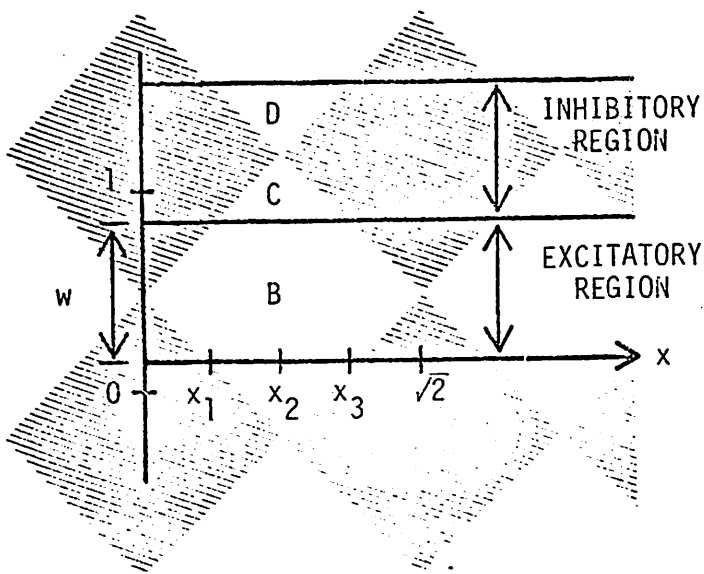
Finally, the area integrated by a diagonally aligned receptive field is given by:

$$A = B - C - D.$$

$A(x)$ is a monotonic increasing, piecewise quadratic function of x , as illustrated in the graph below. A can be approximated by a linear function with slope $1/(2\sqrt{2})$. Substituting $x = r/\sqrt{2}$ and normalizing by rw we obtain:

$$D_2 \approx \frac{1}{2\sqrt{2}}$$

for a receptive field of $w = 1/\sqrt{2}$, aligned diagonally to the pattern.



BIBLIOGRAPHY

- S. Amari and M.A. Arbib, "Competition and cooperation in neural nets," Systems Neuroscience, 1, J. Metzler (ed.), Academic Press, New York (in preparation), 1976.
- H.B. Barlow and J.D. Pettigrew, "Lack of specificity of neurones in the visual cortex of young kittens," J. Physiol., 218, 1971, pp. 98-100P.
- C. Blakemore and F.W. Campbell, "On the existence of neurones in the human visual system selectively sensitive to the orientation and size of retinal images," J. Physiol., 203, 1969, pp. 237-260.
- C. Blakemore and G.F. Cooper, "Development of the brain depends on the visual environment," Nature, 228, 1970, pp. 477-478.
- C. Blakemore and D.E. Mitchell, "Environmental modification of the visual cortex and the neural basis of learning and memory," Nature, 241, 1973, pp. 467-468.
- C. Blakemore, J. Nachmias and P. Sutton, "The perceived spatial frequency shift: evidence for frequency-selective neurones in the human brain," J. Physiol., 210, 1970, pp. 727-750.
- C. Blakemore and P. Sutton, "Size adaptation: a new aftereffect," Science, 166, 1969, pp. 245-247.
- M. Coltheart, "Visual feature-analyzers and after-effects of tilt and curvature," Psychol. Rev., 78, 1971, pp. 114-121.
- O.D. Creutzfeldt, "Some neurophysiological considerations concerning 'memory'," Memory and Transfer of Information, H.P. Zippel (ed.), Plenum Press, New York, 1973, pp. 293-302.
- O.D. Creutzfeldt and P. Heggelund, "Neural plasticity in visual cortex of adult cats after exposure to visual patterns," Science, 188, 1975, pp. 1025-1027.
- M. Cynader, N. Berman and A. Hein, "Cats reared in stroboscopic illumination: effects on receptive fields in visual cortex," Proc. Nat. Acad. Sci., 70, 1973, pp. 1353-1354.
- P. Dev, "Perception of depth surfaces in random-dot stereograms: a neural model," Int. J. Man-Machine Studies, 7, 1975, pp. 511-528.
- R.L. DeValois, I. Abramov and G.H. Jacobs, "Analysis of response patterns of LGN cells," J. Opt. Soc. Am., 56, 1966, pp. 966-977.
- R.L. DeValois and R.T. Marrocco, "Single cell analysis of saturation discrimination in the macaque," Vis. Res., 13, 1973, pp. 701-711.

BIBLIOGRAPHY

- O.E. Favreau, Paper presented at the Canadian Psychological Association Meeting, Toronto, Canada, June, 1976.
- R.D. Freeman and J.D. Pettigrew, "Alteration of visual cortex from environmental asymmetries," Nature, 246, 1973, pp. 359-360.
- A.S. Gilinsky and R.S. Doherty, "Interocular transfer of orientational effects," Science, 164, 1969, pp. 454-455.
- P. Gouras, "Trichromatic mechanisms in single cortical neurons," Science, 168, 1970a, pp. 489-491.
- P. Gouras, "Color sensitive cells in monkey's striate cortex," Fed. Proc., 29, 1970b, p. A838.
- P. Gouras, "Color-opponency from fovea to striate cortex," Invest. Ophthalm., 11, 1972, pp. 427-432.
- P. Gouras, "Opponent-color cells in different layers of foveal striate cortex," J. Physiol., 238, 1974, pp. 583-602.
- M. Green, T. Corwin and V. Zemon, "A comparison of Fourier analysis and feature analysis in pattern-specific color aftereffects," Science, 192, 1976, pp. 147-148.
- S. Grossberg, "Contour enhancement, short-term memory, and constancies in reverberating networks," Studies in Appl. Math., 52, 1973, pp. 213-257.
- S. Grossberg, "Adaptive pattern classification and universal recoding: parallel development and coding of neural feature detectors," Research Report, Boston University, 1975.
- S. Grossberg, "On the development of feature detectors in the visual cortex with applications to learning and reaction-diffusion systems," Biol. Cyb., 21, 1976, pp. 145-159.
- A.R. Hanson, E.M. Riseman and P. Nagin, "Region growing in textured outdoor scenes," Paper presented at the 3rd Milwaukee Symp. on Auto. Comp. and Control, Milwaukee, Wisconsin, April, 1975.
- C.S. Harris, "Effect of viewing distance on a color aftereffect specific to spatial frequency," Psychon. Sci., 21, 1970, p. 350.
- C. Harris, "Orientation-specific color aftereffects dependent on retinal spatial frequency rather than on stripe width," J. Opt. Soc. Am., 61, 1971, p. 689.
- C.S. Harris and A.R. Gibson, "Is orientation-specific color adaptation in human vision due to edge detectors, afterimages, or 'dipoles'?" Science, 162, 1968a, pp. 1506-1507.

BIBLIOGRAPHY

- C.S. Harris and A.R. Gibson, "A minimal model for McCollough's orientation-specific color aftereffect," Paper presented at the Psychon. Sci. Meeting, St. Louis, Missouri, November, 1968b.
- R. Held and S.R. Shattuck, "Color- and edge-sensitive channels in the human visual system: tuning for orientation," Science, 174, 1971, pp. 314-316.
- N. Hepler, "Color: a motion-contingent aftereffect," Science, 162, 1968, pp. 376-377.
- H.V.B. Hirsch and D.N. Spinelli, "Visual experience modifies distribution of horizontally and vertically oriented receptive fields in cats," Science, 168, 1970, pp. 869-871.
- D.H. Hubel and T.N. Wiesel, "Receptive fields, binocular interaction and functional architecture in cat's visual cortex," J. Physiol., 160, 1962, pp. 106-154.
- D.H. Hubel and T.N. Wiesel, "Receptive fields and functional architecture of monkey striate cortex," J. Physiol., 195, 1968, pp. 215-242.
- R.A. Hummel, "Histogram modification techniques," Tech. Report 329, Computer Science Center, University of Maryland, 1975.
- B. Julesz, "Experiments in the visual perception of texture," Sci. Am., 232(4), 1975, pp. 34-43.
- I. Kohler, "Experiments with goggles," Sci. Am., 206(5), 1962, pp. 62-72.
- C.R. Legédy, "Can the data of Campbell and Robson be explained without assuming Fourier analysis?" Biol. Cyb., 17, 1975, pp. 157-163.
- P.K. Leppmann, "Spatial frequency dependent chromatic aftereffects," Nature, 242, 1973, pp. 411-412.
- W.J. Lovegrove and R. Over, "Colour selectivity in orientation masking and aftereffect," Vision Res., 13, 1973, pp. 895-902.
- D.M. MacKay and V. MacKay, "Orientation-sensitive aftereffects of dichoptically presented colour and form," Nature, 242, 1973, pp. 477-479.
- D.M. MacKay and V. MacKay, "What causes decay of pattern-contingent chromatic aftereffects?" Vis. Res., 15, 1975, pp. 462-464.

BIBLIOGRAPHY

- I.D.G. Macleod and A. Rosenfeld, "The visibility of gratings: spatial frequency channels or bar-detecting units?" Vis. Res., 14, 1974, pp. 909-915.
- L. Maffei and A. Fiorentini, "Geniculate neural plasticity in kittens after exposure to periodic gratings," Science, 186, 1974, pp. 447-449.
- L. Maffei, A. Fiorentini and S. Bisti, "Neural correlate of perceptual adaptation to gratings," Science, 182, 1973, pp. 1036-1038.
- J.R.W. Mansfield, "Neural basis of orientation perception in primate vision," Science, 186, 1974, pp. 1133-1135.
- D. Marr, "Analyzing natural images," M.I.T. A.I. Lab. Memo 334, 1975.
- R.H. Masland, "Visual motion perception: experimental modification," Science, 165, 1969, pp. 819-821.
- J.G. May and H.H. Matteson, "Spatial frequency-contingent color after-effects," Science, 192, 1976, pp. 145-147.
- J.E.W. Mayhew and S.M. Anstis, "Movement aftereffects contingent on color, intensity and pattern," Percept. and Psychophys., 12, 1972, pp. 77-85.
- C. McCollough, "Color adaptation of edge-detectors in the human visual system," Science, 149, 1965, pp. 1115-1116.
- J. Metzler and D.N. Spinelli, "Behavioral correlates of physiological changes produced in the activity of single units in the visual cortex of adult cats by restricted, prolonged, visual experience," Brain Res., in preparation, 1976.
- F.S. Montalvo, "Consensus versus competition in neural networks," Int. J. Man-Machine Studies, 7, 1975, pp. 333-346.
- R.B. Morant and J.R. Harris, "Two different aftereffects of exposure to visual tilts," Am. J. Psychol., 78, 1965, pp. 218-226.
- G.M. Murch, "Binocular relationships in size and color orientation specific aftereffect," J. Exp. Psychol., 93, 1972, pp. 30-34.
- G.M. Murch and J.A. Paulson, "Colorimetric matches of McCollough after-effects," Vis. Res., submitted, 1976.
- R. Over, "Comparison of normalization theory and neural enhancement explanation of negative aftereffects," Psychol. Bull., 75, 1971, pp. 225-243.

BIBLIOGRAPHY

- R. Over, N. Long and W. Lovegrove, "Absence of binocular interaction between spatial and color attributes of visual stimuli," Percept. and Psychophys., 13, 1973, pp. 534-540.
- J.D. Pettigrew, "The effect of selective visual experience on stimulus trigger features of kitten cortical neurons," Ann. N.Y. Acad. of Sci., 228, 1974a, pp. 393-405
- J.D. Pettigrew, "The effect of visual experience on the development of stimulus specificity by kitten cortical neurons," J. Physiol., 237, 1974b, pp. 49-74.
- J.D. Pettigrew and R.D. Freeman, "Visual experience without lines: effect on developing cortical neurons," Science, 182, 1973, pp. 599-601.
- L.A. Riggs, K.D. White and P.D. Eimas, "Establishment and decay of orientation-contingent aftereffects of color," Percept. and Psychophys., 16, 1974, pp. 535-542.
- A. Rosenfeld and E.B. Troy, "Visual texture analysis," Symp. on Feature Extraction and Selection in Pattern Recognition, IEEE Publication 70C 51-C, Argonne, Illinois, October, 1970.
- D. Skowbo, T. Gentry, B. Timney and R.B. Morant, "The McCollough effect: influence of several kinds of visual stimulation on decay rate," Percept. and Psychophys., 16, 1974, pp. 47-49.
- D. Skowbo, B.N. Timney, T.A. Gentry and R.B. Morant, "McCollough effects: experimental findings and theoretical accounts," Psychol. Bull., 82, 1975, pp. 497-510.
- D.N. Spinelli, H.V.B. Hirsch, R.W. Phelps and J. Metzler, "Visual experience as a determinant of the response characteristics of cortical receptive fields in cats," Exp. Brain Res., 15, 1972, pp. 289-304.
- D.N. Spinelli and J. Metzler, "The effect of restricted, prolonged, visual experience on the activity of single units in the visual cortex of adult cats," Brain Res., in preparation, 1976.
- C.F. Stromeyer, "Further studies of the McCollough effect," Percept. and Psychophys., 6, 1969, pp. 105-110.
- C.F. Stromeyer, "Edge-contingent color aftereffects: spatial frequency specificity," Vis. Res., 12, 1972a, pp. 717-733.
- C.F. Stromeyer, "Contour-contingent color aftereffects: retinal area specificity," Am. J. Psychol., 85, 1972b, pp. 227-235.
- C.F. Stromeyer and R.J.W. Mansfield, "Colored aftereffects produced with moving edges," Percept. and Psychophys., 7, 1970, pp. 108-114.

BIBLIOGRAPHY

- L.W. Teft and F.T. Clark, "The effects of stimulus density on orientation specific aftereffects of color adaptation," Psychon. Sci., 11, 1968, pp. 265-266.
- B.N. Timney, T.A. Gentry, D. Skowbo and R.B. Morant, "Chromatic grating thresholds and the McCollough effect," Vision Res., 14, 1974, pp. 1033-1035.
- C. von der Malsburg, "Self-organization of orientation sensitive cells in the striate cortex," Kybernetik, 14, 1973, pp. 85-100.
- K.D. White, "Binocular rivalry during establishment of orientation-contingent color aftereffects," Paper presented at the Canadian Psychol. Association Meeting, Toronto, Canada, June, 1976a.
- K.D. White, "Influence of achromatic inspection on McCollough effects," Paper presented at the Assoc. Res. Vis. and Ophthal. Meeting, Sarasota, Florida, 1976b.
- K.D. White, Studies of Orientation-contingent Color Aftereffects, Ph.D. Thesis, Brown University, June, 1976c.
- K.D. White, Personal communication, 1976d.
- T.N. Wiesel and D.H. Hubel, "Single-cell responses in striate cortex of kittens deprived of vision in one eye," J. Neurophysiol., 26, 1963, pp. 1003-1017.
- H.R. Wilson and J.D. Cowan, "A mathematical theory of the functional dynamics of cortical and thalamic nervous tissue," Kybernetik, 13, 1973, pp. 55-80.
- A.L. Zobrist and W.B. Thompson, "Building a distance function of Gestalt grouping," IEEE Trans. Comp., C-4, 1975, pp. 718-728.
- S.W. Zucker, R.A. Hummel, A. Rosenfeld, "Applications of relaxation labelling, 1: line and curve enhancement," Tech. Report 419, Computer Science Center, University of Maryland, 1975.